

REVIEW

Open Access



A review on thermochemical seasonal solar energy storage materials and modeling methods

Abdullah¹, M. Koushaeian¹, N. A. Shah¹ and J. D. Chung^{1*}

Abstract

In the current era, national and international energy strategies are increasingly focused on promoting the adoption of clean and sustainable energy sources. In this perspective, thermal energy storage (TES) is essential in developing sustainable energy systems. Researchers examined thermochemical heat storage because of its benefits over sensible and latent heat storage systems, such as higher energy density and decreased heat loss. Solar energy is a promising alternative among the numerous renewable energy sources. As a result, this study provides an overview of thermochemical heat storage materials, focusing on materials utilized by solar energy systems in buildings. The research examines the storage materials used in relevant studies and the models used to predict and enhance system performance.

Keywords Isotherms, Thermal energy storage, Energy density, Thermochemical materials, Adsorption

1 Introduction

Energy security is a critical concern for every nation's economy, particularly as the global population has grown from 2.5 billion to 8 billion in the past six decades, resulting in a surge in energy demand [1]. The depletion of crude oil reserves has driven the search for alternative energy sources. Researchers and scientists are exploring new renewable, sustainable, eco-friendly, and cost-effective energy sources and systems to meet the rising energy demand. Many developed countries have transitioned from fuel-dependent to renewable and more efficient methods to achieve "Net Zero Emissions by 2050." According to the International Energy Agency (IEA), there was a 50% drop in conventional heating technologies such as coal, oil, and natural gas boilers in 2020.

Furthermore, by 2030, low-carbon district heating and renewables-based heating sales will rise by 80% [2].

The European Union's 2030 Energy Strategy has ambitious goals: reduce greenhouse gas emissions by 30% compared to 1990 levels, raise the renewable energy share to 27% in final energy consumption, and boost energy efficiency by 27%. Building energy performance is vital, as buildings currently contribute 40% of the EU's primary energy consumption and 36% of CO₂ emissions [3]. South Korea is committed to achieving its net-zero goal by 2050 and is investing significantly in developing low-carbon emission technologies. Buildings consume approximately 33% of the electricity produced in South Korea's 2020 energy scenario. To reduce emissions, South Korea intends to model the power system for the period 2034–2035. Flexible resource planning encompasses power plants, grids, demand-side response, and storage technologies [4].

Among different energy storage technologies, thermal energy storage (TES) seems a viable option to reduce electricity consumption in residential buildings for district water heating, space heating, and cooling

*Correspondence:

J. D. Chung

jdchung@sejong.ac.kr

¹ Department of Mechanical Engineering, Sejong University, Seoul, South Korea

applications [5]. The three main types of TES technologies are sensible, latent, and thermochemical [6], as shown in Table 1. The sensible TES system stores energy as sensible heat without any phase transition of the storage material and directly depends on the material-specific heat and temperature difference [7]. Sensible TES systems are more developed and implemented technologies for heating and cooling applications but suffer from high heat loss and large system sizing. Latent TES involves the phase transition of storage material to store energy at a constant temperature. The isothermal process of latent TES contributes notably high storage density compared to sensible TES [8]. The energy storage density for latent TES depends on the material phase change enthalpy and melting temperature. However, drawbacks such as phase separation, subcooling, low thermal conductivity, corrosion, lack of stability, and inflexible heat source temperature restrict latent TES utilization [9].

Though not yet economically practical, thermochemical heat storage systems show great potential due to their unique properties. For heat storage, these devices rely on reversible chemical processes. Heat is delivered to the storage medium during the charging phase, causing an endothermic process. The key benefit here is that the given heat may be kept for a lengthy period with low heat loss as long as the endothermic reaction products stay separated. This, paired with a much greater thermal energy density when compared to sensible and latent heat storage methods, as shown in Fig. 1, makes thermochemical materials (TCM) an appealing alternative for mid-to-long-term heat storage solutions [10].

In the last two decades, considerable research has been carried out on thermochemical TES for short-term and

long-term heat storage applications. Such TES systems exhibit high storage densities and can store thermal energy for extended periods with minimum heat loss [8]. These attributes make thermochemical energy storage a better option than sensible and latent heat storage technologies [9, 10]. Generally, thermochemical TES is categorized into sorption and chemical reactions, as shown in Fig. 2 [11, 12]. The broad term "Sorption" describes the absorption and adsorption phenomenon. "Absorption" is the process where gas-phase molecules are taken up by a liquid or solid, altering its composition. This integration results in a more uniform distribution of the absorbed substance within the medium [13]. The binding of a gas to the surface of a solid or porous object is known as adsorption. There are two types of adsorptions: physisorption and chemisorption. Weaker Van der Waals forces drive physisorption, while chemisorption relies on stronger valence forces, forming more robust bonds. Chemisorption can offer higher thermal energy densities but is often irreversible, making it unsuitable for heat storage.

A typical thermochemical TES is further classified into "Open" and "Close" cycle systems, as shown in Fig. 3 [15]. The open system operates at atmospheric pressure, and the air stream transports sorbate and heat to or out of the sorber bed. In charging/desorption operation, hot, dry air in the sorber bed absorbs the water vapor resulting in cooler and humid air at the bed outlet. Similarly, in discharging/adsorption operation, wet cool air in the bed is adsorbed by storage material, resulting in dry hot air at the bed outlet. A close sorption system is almost like a conventional vapor compression cycle, and a sorber bed replaces only the mechanical compressor, which provides

Table 1 Different types of TES systems [5]

| Attribute | Sensible Heat Storage | Latent Heat Storage | Thermochemical Heat Storage |
|---------------------------------|---|---|---|
| Principle | Thermal energy is stored by increasing the material's temperature without changing its phase Principle: Material specific heat | Thermal energy is stored as the heat of fusion by changing the phase of the material at a sustained temperature Principle: Latent heat of fusion | Thermal energy is stored in an endothermic/exothermic reversible chemical reaction in breaking and reforming molecular bonds Principle: enthalpy and reactant mole numbers |
| Factor affecting energy density | Thermal conductivity Diffusivity Vapor pressure | Thermal conductivity (PCM) Phase precipitation | Reactor design Heat and mass transfer |
| Materials | Solid medium: sand rock, concrete, pebble beds, and bricks Liquid medium: water, molten salts, and Minerals | Paraffin, non-paraffin, Fatty acid, salt hydrates, metals, and eutectic materials | Silica gel, novel porous materials, composite materials, and salt hydrates |
| Storage duration | Small owing to severe heat loss to surroundings | Restricted owing to heat loss | Long with minimum heat loss |
| Energy transport | Short distance | Short distance | Relatively long distance |
| Technology status | Developed | Polite scale | Laboratory and pilot scale |

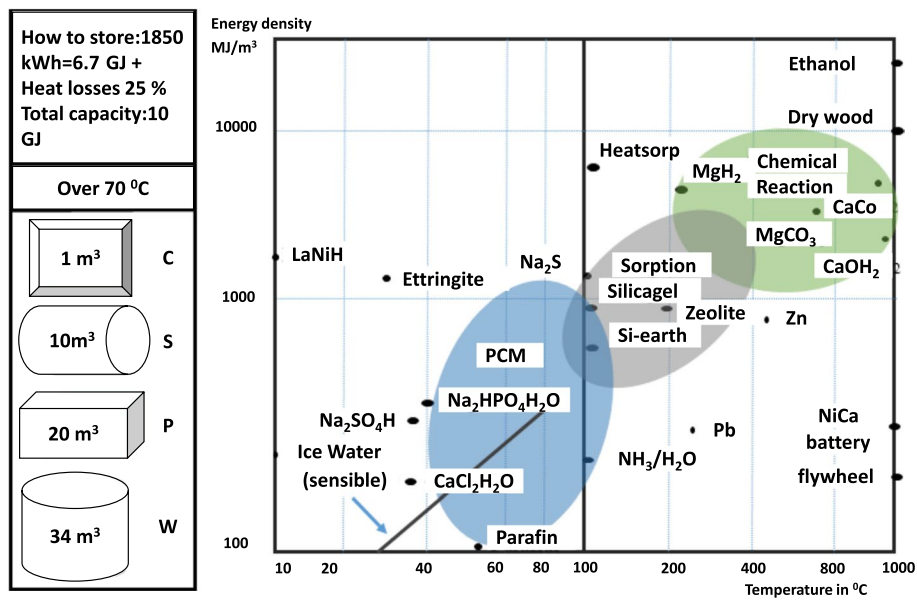


Fig. 1 Energy density comparison of different TES [10]

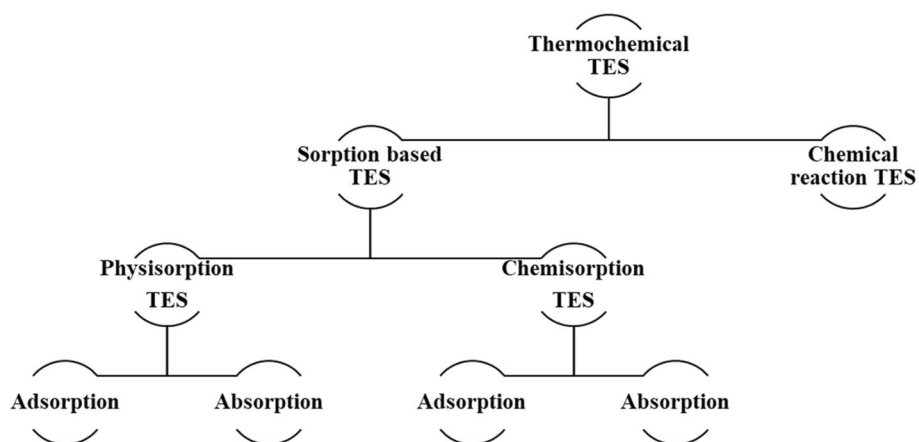


Fig. 2 Classification of sorption TES [14]

the necessary thermal compression to the refrigerant. In the charging/desorption process, hot fluid exchanges heat with the sorber bed, which results in refrigerant desorption, and consequently, the refrigerant is condensed and cooled in the condenser. Similarly, cold fluid cools down the adsorber bed in the discharging process, and the storage material adsorbs refrigerant from the evaporator, releasing heat. This heat can be utilized for space and district water heating applications.

In open systems, only water can be used as sorbate and suffers from poor mass transfer characteristics compared to heat transfer. Furthermore, the bed outlet temperature is restricted by bed thermal mass, which makes the open system more feasible for seasonal TES applications [16].

In contrast, a closed cycle system can use a variety of sorbates and have better mass transfer than heat transfer characteristics [17]. In addition, maintaining a vacuum for extended periods, handling leakage issues, advancing heat exchangers, and providing evaporation heat for heat storage applications are some limiting factors that make the close system feasible only for daily (short-term) heat/cold storage applications.

Thermochemical TES systems are gaining increasing attention due to their high energy density, low operating costs, and ability to store energy for extended periods. The performance of a TES system is influenced by various factors, including the specific TES technology employed, the temperature range within which it

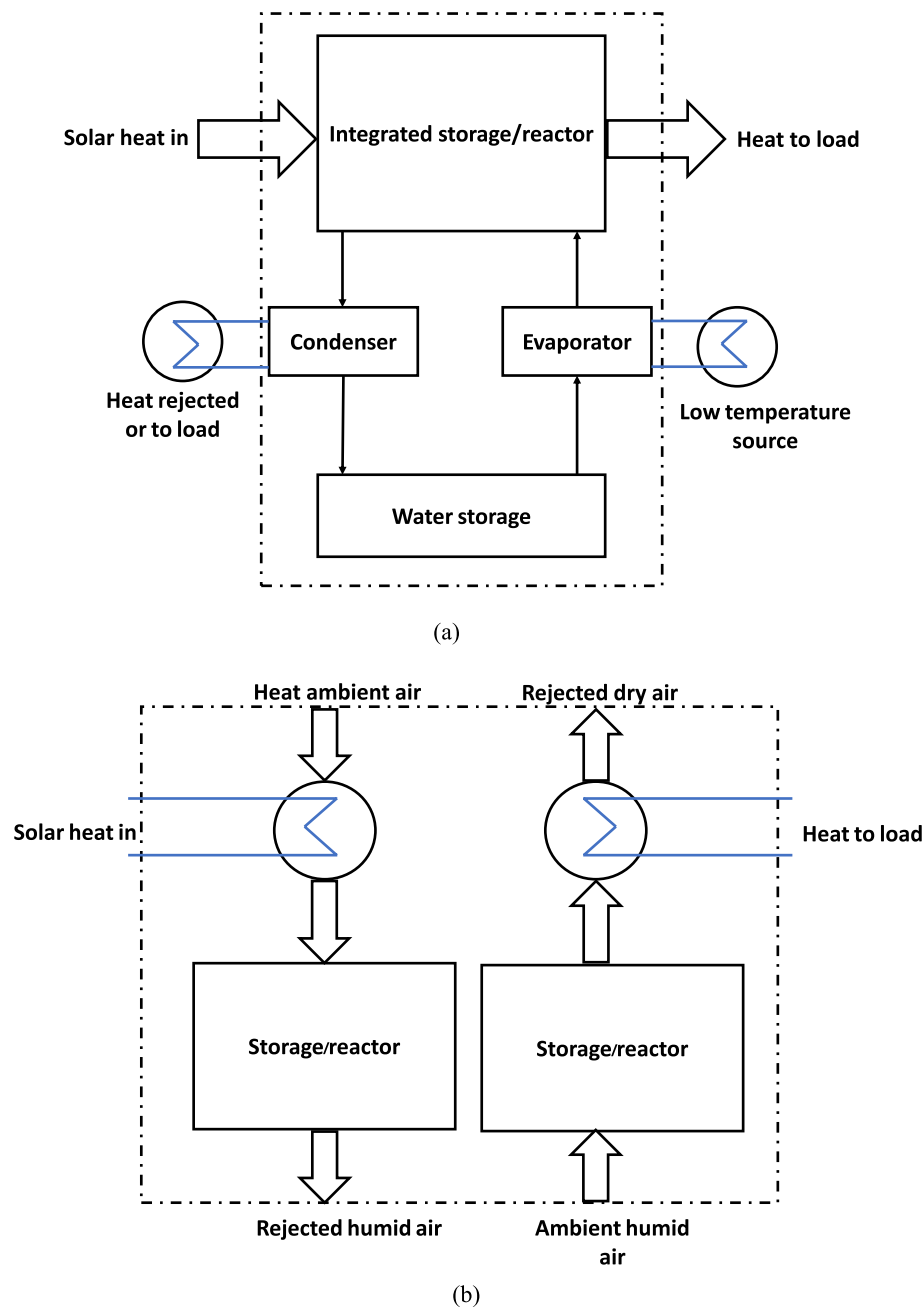


Fig. 3 (a) Closed cycle adsorption system (b) Open cycle system

operates, the duration of storage, and the system’s overall efficiency. The fundamental consideration for a typical thermochemical TES is the type of adsorbent material used, adsorbate (refrigerant), isotherm properties possessed by the adsorbent, and the kinetic model used.

This study examines different thermochemical thermal energy storage (TES) technologies, particularly adsorbent materials used for seasonal heat storage in

solar-powered building systems. This evaluation is confined to thermochemical energy storage devices with charging temperatures less than 140 °C. The primary goal is to offer a comprehensive understanding of the broad spectrum of thermochemical materials (TCMs) used in seasonal heat storage. Furthermore, the study investigates and contrasts various methodologies to improve our understanding of system modeling.

2 Adsorbent materials

Material selection is critical since it significantly influences sorption heat storage design—material qualities, such as structure, size, and thermal properties, impact system efficiency. As a result, while choosing storage materials, particular critical properties must be considered [18, 19]. Choosing appropriate sorption materials depends on several critical characteristics. Indeed, structural factors like porosity and surface area play a substantial role in influencing adsorption and desorption. Higher porosity and surface area improve sorption system efficiency. Material size is crucial, impacting heat transfer rates and performance. Smaller particles boast superior surface area-to-volume ratios, expediting heat transfer [20]. This advantage is particularly beneficial for adsorption-based thermal energy storage, as it accelerates heat transport within the material. The increased surface area enables swift heat absorption from the surroundings, enhancing thermal energy storage effectiveness [21].

The increased surface area also improves the quick distribution of absorbed heat, which is critical for successful energy storage and release in thermal systems. Smaller particles increased surface area-to-volume ratio improves heat absorption, dispersion, and effectiveness in thermochemical energy storage. Thermal characteristics also play an essential role; increased thermal conductivity and specific heat capacity improve heat storage and release efficiency. These parameters work together to provide a powerful sorption heat storage system. Choosing the best sorption materials is critical for designing a successful sorption-based energy storage system [22]. Some vital characteristics of adsorption material for thermal energy storage are given below.

- A. Compactness: Selecting sorption materials with smaller molar volumes can significantly increase the compactness of energy storage devices. Because these materials have less void space between molecules, they can hold more gas in each volume or weight. As a result, energy storage devices composed of such materials have increased storage density, more efficient space use, lower weight, and improved handling. This strategic decision is crucial for applications that need space and weight reduction, such as portable devices, transportation, and industrial settings, emphasizing the importance of low-molar volume sorption materials in compact energy storage systems.
- B. High sorption properties: Choosing materials with good qualities in sorption thermal energy storage systems is critical because they allow for effective charging and discharging. These materials increase energy storage and release capabilities, resulting in compact and efficient systems. High sorption qualities improve energy storage efficiency, allow quick energy release, and assure system longevity. This option has advantages such as a smaller system footprint, a longer operational lifespan, application adaptability, and environmental friendliness, making it critical for successful thermal energy management and sustainable energy solutions.
- C. Maximum energy density: sorption thermal energy storage uses reversible chemical or physical changes to bind gas to sorption materials at low temperatures and release it at higher temperatures. The material capacity, operating temperatures, favorable adsorption isotherms, and customized features influence energy density, measured as stored energy per unit volume. More significant energy storage potential is enabled by larger adsorption capacity, which is best achieved at lower operating temperatures for effective gas binding. A positive adsorption isotherm, in which gas binds effectively under desirable circumstances, and enhanced physical and chemical adsorbent characteristics such as increased surface area and specific gas affinity boost energy density even more. Finally, choosing a material with a large capacity and perfect properties for the desired temperature increases energy density, providing efficient and space-effective thermal energy storage.
- D. Small volume changes: sorption thermal energy storage attaches and detaches molecules from the surface of a solid substance to store and release thermal energy. It is critical to use materials with low-volume changes throughout these procedures. This option protects the structural stability of the system over time, as considerable volume shifts might cause material fatigue and failure due to mechanical stress. Furthermore, by decreasing wear and tear caused by repetitive heat cycling, materials with minimal volume fluctuations enhance the lifespan of the energy storage system, assuring dependable and efficient operation for the entirety of its operational life. Choosing such materials, in essence, protects the system's integrity, performance, and durability throughout thermal energy storage operations.
- E. High thermal conductivity: Sorption Thermal Energy Storage (STES) system stores thermal energy by adsorbing/absorbing and desorbing a working fluid onto a solid/liquid absorbent. Thermal qualities, notably high thermal conductivity in the adsorbent material and the working fluid are critical to STES efficiency. This conductivity speeds up heat transport, allowing faster energy storage and release cycles. Rapid temperature responses are assured, which is critical for applications that require rapid

energy transfers. Heat distribution is improved, which is critical for optimizing material capacity. High conductivity reduces inefficiencies caused by localized overheating by reducing thermal gradients. Energy losses are minimized, as effective heat transfer reduces wastage. Furthermore, this trait allows for more compact system designs, which may result in cost savings. Thermal conductivity, stability, adsorption/desorption characteristics, and cost are all elements to consider when designing an efficient STES system.

- F. Low regeneration time: Low regeneration time in Sorption Thermal Energy Storage (STES) denotes the quick recovery of stored thermal energy as materials release heat during desorption. This quick regeneration cycle, made possible by materials with excellent adsorption/absorption and desorption properties, lowers downtime between energy release and capture phases. As a result, the STES system becomes extremely responsive, eliminating idle time, maximizing energy use, and improving overall operational efficiency for quickly addressing variable heating or cooling requirements in applications such as industrial processes and HVAC systems.
- G. High heat and mass transport: High heat and mass transport rates are critical for enhancing the efficiency of the STES system. Rapid charging and discharging operations are ensured by efficient heat transfer inside the sorbent material and good thermal conductivity at heat exchange interfaces, lowering cycle durations and increasing total system efficiency. Similarly, more excellent mass transfer rates enable faster adsorption and desorption, allowing the system to quickly adapt to changing energy demands. These variables result in advantages such as increased system control, smaller designs, and greater integration into various applications, making STES a more effective and feasible alternative for sustainable energy management.
- H. Non-corrosive and non-flammable: Using non-corrosive and non-flammable sorption materials is critical in STES. These properties are critical for assuring the energy storage system's endurance and safety. Non-corrosive materials protect the system from deterioration and possible interactions with the adsorbed fluid. On the other hand, non-flammable materials remove the possibility of igniting during adsorption or desorption processes, protecting against fires and explosions. STES systems prioritizing these characteristics can function consistently, effectively, and securely, contributing to sustainable energy solutions.
- I. High reaction output: High reaction output in Sorption Thermal Energy Storage (STES) refers to the

ability of sorption materials to capture and discharge thermal energy efficiently throughout the charge and discharge cycles. Reversible adsorption and desorption of a sorbate, such as water vapor, onto a solid sorbent is essential in STES. The efficacy of STES is dependent on the properties of sorption materials. Sorption materials with high reaction output have strong adsorption/absorption capabilities, allowing for significant heat buildup. High reaction output sorption materials effectively discharge significant heat during this process, increasing energy yield. Optimal sorption materials with high reaction output exhibit effective adsorption and desorption characteristics due to high capacity, optimal pore designs, and favorable thermodynamic properties. This improves energy storage and release performance, elevating the entire STES system.

Selecting the optimal material for heat storage systems can be challenging due to the difficulty of finding a single material that possesses all the desired properties. Choosing the optimal material for heat storage systems can be challenging since finding a single material that encompasses all the desired properties is challenging. However, among the properties listed above, sorption energy and energy density are essential considerations. Sorption properties, such as adsorption/absorption and desorption capacity, play a critical role in determining the effectiveness of heat storage systems. The ability of a material to store and release thermal energy depends on its sorption properties. Selecting materials with strong sorption properties is crucial for efficient heat storage systems. Energy density is equally vital, measuring how much energy a material can store per unit volume or mass. High-energy-density materials excel at storing more thermal energy, enhancing their effectiveness in heat storage applications.

Water is the chosen material for seasonal solar energy storage in buildings due to its environmental friendliness and cost-effectiveness. As a result, hydrophilic materials are useful as sorbents. Silica gels are widely studied hydrophilic compounds because of their high attraction to water vapor, considerable water absorption capability at low humidity levels, affordability, and ease of regeneration. Task 32 of IEA-SHC (International Energy Agency-Solar Heating and Cooling) is a noteworthy experimental study for heat storage applications [23]. For instance, SPF [24] and MODESTORE [25] projects examined the closed cycle system for silica gel-water and zeolite 13X-water pairs with energy storage densities of 33.3 kWh/m³ and 57.8 kWh/m³, respectively. TCA (Thermo-Chemical Accumulator) is a prominent IEA-SHC project among prototypes developed. This experimental result

reveals a high material-based energy storage density of 253 kWh/m³, while a lower reported value of 85kWh/m³ for the system/prototype.

Li et al. [26] performed an experimental study to evaluate energy and exergy performance for an adsorption heat storage system. This study was performed for FAM-Z01 and water as working pairs with reported energy storage densities of 805 kJ/kg. Deshmukh et al. [27] designed a closed-cycle system that utilizes a silica gel-water pair with a heat storage capacity of 18 kWh. This system can deliver 3 kWh of thermal energy over 6 h. It achieves a storage density of 42 kWh/m³ by employing 350 kg of adsorbent material. Additionally, the heat exchanger within the system has a capacity of 400 W/K. ATES have higher energy densities than other technologies (latent and sensible TES); such systems still suffer from poor thermodynamic efficiency, and technology status is under research. Table 2 provides information on energy storage densities and the temperatures required for charging and discharging a range of thermochemical heat storage materials. Materials that exhibit lower charging temperatures and higher energy storage densities are promising candidates for practical applications in thermochemical heat storage.

These highly desirable materials offer efficient energy storage for diverse applications and advance

sustainable, eco-friendly energy systems. Water is often recommended for seasonal solar energy storage in buildings due to its cost-effectiveness and ecological benefits. Hydrophilic materials with rapid water absorption, such as silica gels, are excellent sorbents. Silica gels are an excellent choice for thermochemical energy storage. They have a strong affinity for water vapor, a high water absorption capacity even in low humidity conditions, and are cost-effective. Additionally, they are easy to regenerate, making them an attractive option for this purpose. Extensive research supports their significant potential for storing seasonal solar energy in buildings.

Silica gels have a notable limitation regarding their low hydrophilic characteristics within the operational range, resulting in low material energy densities. Consequently, the potential utilization of silica gels in solar energy storage remains uncertain. Compared to silica gels, zeolites have increased hydrophilicity due to the strong interaction between their electrostatically charged structure and water molecules [68]. As a result, zeolites require higher temperatures for charging or desorption, which may be customized using dealumination, ion exchange, or changes in the aluminum–silicon ratio [104]. To improve mass and heat transfer performance, a different approach involves incorporating hygroscopic salts into mesoporous silicates. However, the presence of salts causes salt

Table 2 Conventional adsorbent for heating applications

| Principle | Sorbent/sorbate | Desorption Temperature (°C) | Adsorption Temperature (°C) | Energy Density (kWh/m ³) | References |
|-------------------|--|-----------------------------|-----------------------------|--------------------------------------|-----------------|
| Adsorption | Silica gel/ H ₂ O | 88 | 32 | 50–125 | [20, 21, 24–36] |
| | Zeolite 13X/ H ₂ O | 160–180 | 20–40 | 97–160.5 | [17, 36–53] |
| | Zeolite 4A/ H ₂ O | 180 | 65 | 130–148 | [38, 54–59] |
| | Zeolite 5A/ H ₂ O | 80–120 | 20–30 | 83 | [60–62] |
| | Zeolite MSX/ H ₂ O | 230 | - | 154 | [58, 63] |
| | APO-n/ H ₂ O | 95–140 | 40 | 240 | [40, 63–68] |
| | SAPO-n/ H ₂ O | 95–140 | 40 | - | [40, 63–67] |
| | MeAPO-n/ H ₂ O | 95–140 | 40 | - | [63–65, 68] |
| Absorption | CaCl ₂ / H ₂ O | 45–138 | 21 | 118–378 | [69–74] |
| | LiCl/ H ₂ O | 66–87 | 30 | 254–398 | [24, 70] |
| | LiCl ₂ / H ₂ O | 46–87 | 30 | 254 | [20, 24, 75] |
| | LiBr/ H ₂ O | 40–90 | 30 | 252–313 | [70, 76–80] |
| | NaOH/ H ₂ O | 50–95 | 70 | 156–252 | [24, 70, 81–88] |
| | SrBr ₂ / H ₂ O | 80 | - | 62–324 | [89–94] |
| Chemical reaction | CaSO ₄ / H ₂ O | - | 89 | 394 | [11] |
| | CuSO ₄ / H ₂ O | 92 | - | 576 | [95] |
| | Li ₂ SO ₄ / H ₂ O | 103 | - | 252 | [95] |
| | MgCl ₂ / H ₂ O | 130–150 | 30–50 | 555–696 | [72, 96, 97] |
| | MgSO ₄ / H ₂ O | 122–150 | 120 | 422–926 | [8, 98] |
| | Na ₂ S/ H ₂ O | 80–95 | 85–115 | 784 | [99–103] |

species to leak and makes these composite materials vulnerable to corrosion [105].

As to specific examinations, microporous APO-n, SAPO-n, and MeAPO-n can change zeolites [106, 107]. These modifications offer advantages such as lower discharging temperatures and higher energy densities [40, 63–68]. Researchers have primarily focused on enhancing the uptake of sorbate (water) for heat storage applications by incorporating silicon or metal cations into aluminophosphates [67, 108, 109]. Even yet, after a few charging and discharging cycles, the performance of these compounds starts to decline due to framework structure degradation and cation dislodgement [110]. Nonetheless, in contrast with zeolites (and silica gels), the high price of aluminophosphate synthesis is a considerable drawback [8, 44, 111].

Calcium chloride (CaCl_2), lithium chloride (LiCl), lithium bromide (LiBr), and sodium hydroxide (NaOH) are often utilized as reactive sorbents in absorption heat storage studies, using water as the sorbate. NaOH is classified as a strong base, whereas the remaining substances are hygroscopic salts typically employed in solution form. Strong acids and bases are advantageous due to their exceptional water absorption properties and cost-effectiveness. They are, however, caustic and need high charging temperatures. Chemical reactions are distinct from sorption processes in that they include a change in the molecular structure of the substances. While chemical processes offer promise for energy storage at the material level, their practical efficacy requires further research. Deliquescence, swelling, and agglomeration impede long-term responses beyond early cycles [112]. Furthermore, volume changes in materials during chemical reactions can cause hysteresis. Sorption processes, which need less activation energy than chemical reactions, are better suited for low-temperature applications such as seasonal solar energy storage. In addition, due to corrosion and crystallization concerns with liquid–gas absorption systems, only heat storage applications employing solid–gas adsorption techniques are explored in the following section.

3 Modeling methods

Computational models based on sorption material properties can be used to develop and simulate sorption storage systems. This approach enables the storage system's design to be optimized and its performance at an application size to be evaluated without the need for costly experimental experiments. Numerical models may be used to create and model sorption storage systems, allowing full-scale studies to evaluate the most promising storage techniques and materials. Spatially resolved models, lumped-parameter, and Steady-state are the

three methods used in simulating solid–gas adsorption processes. These numerous modeling approaches capture the dynamics and behavior of adsorption systems to varying depths and precision.

Steady-state models assume thermodynamic equilibrium between the adsorbate and adsorbent to calculate the upper-performance limit of a storage system, disregarding heat and mass transfer kinetics within the adsorbent bed. Lumped-parameter models are more exact than steady-state models and may be used to scale the reactor or estimate its overall performance in various scenarios. Spatially resolved models, on the other hand, are required for precise modeling and optimization of reactor operations. Spatially resolved models provide superior resolution and detailed insights into variable distribution and events within the system. They account for heat and mass movement, considering temporal and spatial changes in state variables like temperature gradients in the adsorbent bed during the entire process. However, using geographically resolved models has the disadvantage of necessitating the solution of complicated boundary conditions and transient, spatially coupled heat and mass transfer balance equations. This necessitates the use of specific numerical methods such as the finite difference method (FDM), finite element method (FEM), and finite volume method (FVM).

3.1 Isotherms

To quantify the quantity of vapor adsorption by the adsorbent at a given temperature and pressure, all the modeling methodologies for solid–gas adsorption processes listed above require an equilibrium isotherm. Adsorption equilibrium is when a gas or vapor saturates an adsorbent's surface in specific pressure and temperature circumstances. This state of equilibrium could be described as follows:

$$q = f(P, T)$$

where q is the amount of adsorbate per unit weight of adsorbent, P denotes the equilibrium pressure, and T denotes the absolute temperature. There are three methods for expressing adsorption equilibrium:

1. Adsorption Isotherm: An adsorption isotherm describes the relationship between adsorbate quantity and pressure while the adsorbent temperature remains constant, and the gas pressure varies $q=f(P)$ at constant T
2. Adsorption Isobar: When the gas pressure is held constant while the adsorbent temperature fluctuates, the adsorbate amount-temperature relation is described as an adsorption isobar: $q=f(T)$ at constant P

3. Adsorption Isostere: When the quantity of adsorbate remains constant, the pressure–temperature relation characterized as an adsorption isostere: $P=f(T)$ when q is constant

In applied adsorption research, isotherms are commonly used to represent the results, while isobars and isosteres are less frequently employed. Adsorption isotherms show how the amount of adsorbate changes as the gas pressure changes at a constant temperature. Several mathematical models and theories have been developed to characterize adsorption isotherms [113]. Many of these models are empirical and rely on experimental data to establish correlations between two or more empirical factors. Unlike other methodologies, empirical equations frequently represent experimental data more precisely. Numerous equilibrium isotherm models, including Langmuir, Freundlich, BET, Redlich-Peterson, Dubinin-Radushkevich, Temkin, Toth, Koble-Corrigan, Sips, Khan, Hill, Flory–Huggins, and Radke-Prausnitz, have emerged from three fundamental approaches. These models provide distinct mathematical descriptions of adsorbate interactions with adsorbents in adsorption processes [114]. The first approach, Kinetic Consideration, defines adsorption equilibrium as a dynamic state where adsorption and desorption rates are equal [115]. The second approach, Thermodynamics, is a foundation for deriving various adsorption isotherm models [116, 117]. The third approach, Potential Theory, focuses on generating characteristic curves [118]. A noteworthy trend in isotherm modeling has emerged, encompassing various approaches that result in differences in the understanding of model parameters [119].

3.1.1 Two parameter models

Two-parameter isotherms are mathematical models that describe the adsorption of a solute onto a solid surface or the sorption of gases or liquids onto porous materials. These isotherms relate the equilibrium concentration of the adsorbate on the adsorbent to the pressure or concentration of the adsorbate in the gas or liquid phase.

3.1.2 Langmuir isotherm model

The Langmuir adsorption isotherm, developed initially for gas–solid-phase adsorption onto activated carbon, is commonly used to evaluate and compare different biosorbents. This empirical model assumes a monolayer adsorption scenario with a single-molecule-thick layer on the surface. Adsorption is limited to specific, identical sites, free from lateral interactions or steric hindrance among neighboring adsorbed molecules [120]. In the Langmuir isotherm, homogeneous adsorption is considered, with each molecule having constant enthalpies and

sorption activation energy, indicating that all sites possess equal affinity for the adsorbate [121]. Furthermore, the adsorbate is not transmitted within the surface plane [122, 123]. The Langmuir adsorption isotherm graphically exhibits a plateau, representing an equilibrium saturation point [124], where further adsorption is prevented once a molecule occupies a site [125, 126]. Langmuir's theory correlates the rapid decrease in intermolecular attractive forces with increased distance. The mathematical expression of the Langmuir isotherm is outlined in Table 3. The Langmuir isotherm introduces a dimensionless constant, referred to as the separation factor (R_L), initially defined by Webber and Chakkravorti [127]. This factor can be expressed as:

$$R_L = \frac{1}{1 + K_L C_0} \quad (1)$$

Here, K_L (L/mg) stands for the Langmuir constant, and C_0 represents the initial concentration of the adsorbate (mg/L). A lower R_L value suggests more favorable adsorption. In a more detailed interpretation, the R_L value characterizes the nature of adsorption as unfavorable ($R_L > 1$), linear ($R_L = 1$), favorable ($0 < R_L < 1$), or irreversible ($R_L = 0$).

3.1.3 Freundlich isotherm model

The Freundlich isotherm, introduced by Freundlich [141], is one of the earliest models for describing non-ideal and reversible adsorption, and it is not limited to monolayer formation. This empirical model is suitable for multilayer adsorption scenarios, where the distribution of adsorption heat and affinities across a heterogeneous surface is non-uniform [142]. Historically, it was developed for the adsorption of animal charcoal, highlighting that the ratio of adsorbate to adsorbent mass was not constant at different solution concentrations [125]. In this context, the total adsorbed amount is the cumulative result of adsorption at individual sites, each with its distinct bond energy. Initially, the stronger binding sites are filled, and as the process continues, the adsorption energy steadily decreases, following an exponential trend [126]. Today, the Freundlich isotherm finds widespread use in heterogeneous systems, particularly for organic compounds or highly interactive species on activated carbon and molecular sieves. The slope, which ranges between 0 and 1, measures adsorption intensity or surface heterogeneity, with values closer to zero indicating more significant surface heterogeneity. The slope below unity implies a chemisorption process, while a value above one suggests cooperative adsorption [143]. Linearized and non-linearized equations for the Freundlich isotherm can be found in Table 3. The Freundlich isotherm has come under scrutiny recently due to its absence of a

Table 3 Summary of isotherm models

| Isotherm | Nonlinear form | Reference |
|---|---|-----------|
| Two parameter isotherms | | |
| Langmuir | $q_e = \frac{Q_0 b C_e}{1 + b C_e}$ | [115] |
| Freundlich | $q_e = K_F C_e^{1/n}$ | [128] |
| Dubinin-Radushkevich | $q_e = q_s \exp(-k_{ad} \epsilon^2)$ | [129] |
| Temkin | $q_e = \frac{RT}{b_T} \ln A_T C_e$ | [130] |
| Flory-Huggins | $\frac{\theta}{C_0} = K_{FH} (1 - \theta)^{n_{FH}}$ | [131] |
| Hill | $q_e = \frac{q_{st} C_e^{n_H}}{K_D + C_e^{n_H}}$ | [132] |
| Three parameter isotherms | | |
| Redlich-Peterson | $q_e = \frac{K_R C_e}{1 + a_R C_e^g}$ | [133] |
| Sips | $q_e = \frac{K_S C_e^{\beta S}}{1 + a_S C_e^{\beta S}}$ | [134] |
| Toth | $q_e = \frac{K_T C_e}{(a_T + C_e)^{1/t}}$ | [135] |
| Koble-Corrigan | $q_e = \frac{A C_e^n}{1 + B C_e^n}$ | [136] |
| Khan | $q_e = \frac{q_s b_K C_e}{(1 + b_K C_e)^{a_K}}$ | [137] |
| Radke-Prausnitz | $q_e = \frac{a_{RP} r_R C_e^{\beta_R}}{a_{RP} + r_R C_e^{\beta_R - 1}}$ | [120] |
| Multilayer physisorption isotherms | | |
| BET | $q_e = \frac{q_s C_{BET} C_e}{(C_s - C_e) [1 + (C_{BET} - 1) (C_e / C_s)]}$ | [138] |
| FHH | $\ln \left(\frac{C_e}{C_s} \right) = - \frac{\alpha}{RT} \left(\frac{q_s}{q_e a} \right)^f$ | [139] |
| MET | $q_e = q_s \left(\frac{k}{\ln(C_s / C_e)} \right)^{1/\beta}$ | [140] |

fundamental thermodynamic foundation and failure to converge to Henry’s law at low concentrations, which is worth noting [144].

3.1.4 Dubinin–Radushkevich isotherm model

The Dubinin–Radushkevich (D-A) model [129] was initially formulated to model subcritical vapor adsorption on micropore solids, focusing on the pore-filling mechanism. This model is frequently employed for explaining the adsorption process [145], incorporating a Gaussian energy distribution on a heterogeneous surface [54]. This model often fits well for high solute activities and intermediate concentration ranges but lacks satisfactory asymptotic properties and doesn’t predict Henry’s law at low pressures [146]. This approach is frequently employed to differentiate between metal ions’ physical and chemical adsorption [118]. It calculates the mean free energy, E per molecule of adsorbate, required to remove a molecule from its position in the sorption space to infinity using the equation:

$$E = \left[\frac{1}{\sqrt{2B_{DR}}} \right] \tag{2}$$

Here, B_{DR} represents the isotherm constant. Additionally, the parameter ϵ can be correlated as:

$$\epsilon = RT \ln \left[1 + \frac{1}{C_e} \right] \tag{3}$$

In this equation, R, T, and C_e denote the gas constant (8.314 J/mol K), absolute temperature (K), and adsorbate equilibrium concentration (mg/L), respectively. One distinctive feature of the Dubinin–Radushkevich isotherm is its temperature dependence.

3.1.5 Temkin isotherm model

The Temkin isotherm, developed initially to describe hydrogen adsorption onto platinum electrodes in acidic solutions, incorporates a factor that explicitly considers adsorbent-adsorbate interactions [147]. This model simplifies the behavior by assuming that the heat of adsorption (which depends on temperature) decreases linearly rather than logarithmically, with coverage [148]. The equation suggests an even distribution of binding energies, reaching a maximum binding energy. The Temkin equation proves helpful in forecasting gas-phase equilibrium, particularly in scenarios where a closely arranged

structure with uniform orientation is not required. However, it may not be suitable for intricate adsorption systems, mainly when dealing with liquid-phase adsorption isotherms [149].

3.1.6 Flory–Huggins isotherm model

The Flory–Huggins isotherm model [131], at times, used to determine the degree of surface coverage of an adsorbate on an adsorbent, helps express the feasibility and spontaneity of an adsorption process. In this context, θ represents the degree of surface coverage, while K_{FH} and n_{FH} are indicators of its equilibrium constant and model exponent. The equilibrium constant, denoted as K_{FH} , used for calculating the Gibbs free energy of spontaneity, is associated with the equation [120]:

$$\Delta G_0 = -RT \ln(K_{FH}) \quad (4)$$

3.1.7 Three parameter models

Three-parameter isotherms are equations used to describe the adsorption of solutes onto adsorbents. They involve three parameters to account for additional complexities in the adsorption process, offering greater flexibility in fitting experimental data compared to two-parameter models. These models often introduce an extra parameter, such as a shape parameter or an exponent, to improve the accuracy of adsorption predictions. The choice of a specific three-parameter isotherm depends on the nature of the adsorption system and the available experimental data.

3.1.8 Redlich–Peterson isotherm model

The Redlich–Peterson isotherm [133] is a versatile model combining Langmuir and Freundlich isotherms elements, incorporating three parameters into its empirical equation [150]. This model features a linear concentration term in the numerator and an exponential function in the denominator [151], allowing it to describe adsorption equilibria across a broad concentration range. Due to their flexibility, they can be applied to both homogeneous and heterogeneous systems [152]. Model parameters are typically obtained through a minimization process that maximizes the correlation coefficient between experimental data and theoretical predictions. This is often achieved using solver add-in functions in software like Microsoft Excel [153]. In terms of behavior, at high concentrations, the Redlich–Peterson isotherm approaches the Freundlich isotherm model (as the exponent β tends to zero), and in the low concentration limit, it aligns with the ideal Langmuir condition (as the β values are all close to one) [151].

3.1.9 Sips isotherm model

The Sips isotherm [134] is a composite model combining elements from the Langmuir and Freundlich expressions. It is specifically designed to predict adsorption behavior in heterogeneous systems [145] and overcome the limitations associated with the Freundlich isotherm, which fails to describe adsorption at rising adsorbate concentrations. At low adsorbate concentrations, the Sips isotherm reduces to the Freundlich model, while at high concentrations, it predicts a monolayer adsorption capacity characteristic of the Langmuir isotherm. In practice, the operating conditions influence the Sips isotherm equation parameters [122].

3.1.10 Toth isotherm model

The Toth isotherm [135] serves as an empirical equation intended to improve the fitting of Langmuir isotherms when working with experimental data. It is a valuable tool in characterizing heterogeneous adsorption systems, effectively addressing low and high-end concentration boundaries [120]. This model assumes an asymmetrical quasi-Gaussian energy distribution, where most adsorption sites have energies lower than the peak or mean value [144].

3.1.11 Koble–Corrigan isotherm model

The Koble–Corrigan model [136] is a three-parameter equation like the Sips isotherm model. The constants of the isotherm, identified as A, B, and n, are usually derived through a trial-and-error optimization approach, often involving linear plots.

3.1.12 Khan isotherm model

The Khan isotherm [137] is primarily recommended for pure solutions, with two parameters: b_K , representing the model constant, and a_K , signifying the model exponent. This model excels when it attains high correlation coefficients and minimizes ERRSQ or chi-square values, facilitating precise determination of maximum uptake values [154].

3.1.13 Radke–Prausnitz isotherm model

The Radke–Prausnitz isotherm is often well correlated with high RMSE and chi-square values. A model exponent characterizes it as β_R , with the constants a_R and r_R playing essential roles in the equation [120].

The Brunauer–Emmett–Teller (BET) isotherm [138] is a theoretical equation primarily applied in gas–solid equilibrium systems. It was developed to describe multilayer adsorption systems within a specific relative pressure range (0.05 to 0.30), corresponding to

monolayer coverage between 0.50 and 1.50. Its equation for liquid–solid interfaces is as follows:

$$q_e = \frac{q_s C_{BET} C_e}{(C_s - C_e) [1 + (C_{BET} - 1)(C_e/C_s)]} \quad (5)$$

In Eq. (5), C_{BET} , C_s , q_s , and q_e represent the BET adsorption isotherm (L/mg), adsorbate monolayer saturation concentration (mg/L), theoretical isotherm saturation capacity (mg/g), and equilibrium adsorption capacity (mg/g), respectively. When C_{BET} and $C_{BET}(C_e/C_s)$ are significantly greater than 1, the equation simplifies to:

$$q_e = \frac{q_s}{1 - (C_e/C_s)} \quad (6)$$

Additionally, the Frenkel-Halsey-Hill (FHH) isotherm [139], derived from potential theory, can be expressed as:

$$\ln\left(\frac{C_e}{C_s}\right) = -\frac{\alpha}{RT} \left(\frac{q_s}{q_e d}\right)^r \quad (7)$$

Here, d , α , and r represent the interlayer spacing, isotherm constant, and the inverse power of distance from the surface. Similarly, the MacMillan-Teller (MET) isotherm [140], which incorporates surface tension effects in the BET isotherm, is written as:

$$q_e = q_s \left(\frac{k}{\ln(C_s/C_e)} \right)^{1/3} \quad (8)$$

where k is an isotherm constant. When C_s/C_e approaches unity, the logarithmic term can be approximated as:

$$q_e = q_s \left(\frac{C_e k}{C_s - C_e} \right)^{1/3} \quad (9)$$

As a note, the empirical isotherm is a reasonable fit for Frenkel-Halsey-Hill (FHH) or MacMillan-Teller (MET) isotherms when the relative pressures are higher than 0.8, and it approximates the Brunauer–Emmett–Teller (BET) isotherm for relative pressures lower than 0.35. Adsorption equilibria are commonly described using the Langmuir isotherm [155], BET isotherm [138], Tòth isotherm [135], and the Dubinin–Polanyi (DP) theory [156] Table 3. The Dubinin–Polanyi (DP) theory is widely utilized in modeling techniques to explain adsorption equilibria since it permits the derivation of all isolines from a single characteristic curve. The Dubinin–Radushkevich (DR) equation [129] and its generalization, the Dubinin–Astakhov (DA) equation [157], are widely used expressions for fitting experimentally obtained characteristic curves.

The Dubinin–Polanyi theory requires the adsorbate density function as a crucial parameter, which explains

the temperature dependence of the adsorbate density necessary for calculating the adsorbent loading and adsorption enthalpy. Cook et al. [158] and Nikolaev et al. [159] have proposed various density functions but were not widely favored. Lehmann et al. [50] have investigated the problem of selecting an appropriate adsorbate density function, and Nagel et al. [160]. In their studies, a comparison was made among different density models. Lehmann et al. [50] suggested that simpler density models should be preferred as they have little effect on the resulting heat storage densities, thus improving computational efficiency. On the other hand, Nagel et al. [161] advocated employing a comprehensive mathematical expression to generate an acceptable fit of the experimentally collected characteristic curve for energy storage applications. They also proposed utilizing a linear density model in this circumstance.

3.2 Adsorption kinetics

Adsorption isotherms depict an adsorbent's equilibrium vapor uptake as a function of adsorbent bed characteristics such as temperature and pressure. On the other hand, non-equilibrium conditions may result in a divergence between the actual and maximum vapor uptakes, which governs the rate of adsorptions. Typically, kinetics modeling can be explained by Fickian diffusion [162], the linear driving force (LDF) model [163], or its modified form. Fickian diffusion and the Linear Driving Force (LDF) model are distinct approaches to understanding mass transfer processes, including adsorption. Fickian diffusion is a fundamental, mechanistic model that describes the movement of molecules based on concentration gradients and is suitable for situations with significant concentration differences. In contrast, the LDF model is an empirical approach that assumes mass transfer is proportional to the difference between the equilibrium and actual concentrations. It is used when systems are near equilibrium and concentration gradients are small. The choice between these models depends on the specific conditions of the system, with Fickian diffusion providing a detailed description of diffusion and the LDF model simplifying modeling for near-equilibrium situations. Depending on the system, a combination of both models may be required for a comprehensive analysis.

3.2.1 Fickian diffusion in a spherical particle

Concentration behavior within a homogeneous sphere of radius 'a' over time, governed by Fick's law for isothermal diffusion with a diffusivity constant 'D', can be analyzed to provide insights into short-term and long-term concentration changes [164].

$$\frac{\delta C}{\delta t} = D \left(\frac{\delta^2 C}{\delta a^2} + \frac{2\delta C}{r\delta a} \right) \quad (10)$$

The solution of this equation is:

$$\frac{M_t}{M_\infty} = 1 - \frac{6}{\pi^2} \sum_{n=1}^{\infty} \left(\frac{1}{n^2} \right) \exp\left(-\frac{Dn^2\pi^2 t}{a^2}\right) \quad (11)$$

where M_t = gas uptake at time t and M_∞ = gas uptake at equilibrium. For small times the solution reduces to

$$\frac{M_t}{M_\infty} = \frac{6D^{1/2} t^{1/2}}{\pi^{1/2} a} \quad (12)$$

The primary challenge with this approach is the reduced accuracy of experimental data during the initial uptake period, owing to practical limitations, such as finite gas exchange times [165]. Equation (11) involves a rapidly converging series with the diffusion coefficient 'D' and time 't' as complementary parameters. These parameters yield a dimensionless time parameter specific to a given particle size. Using Eq. (11) to model Fickian diffusion into a spherical particle, one can generate graphs of $\ln(1 - M_t/M_\infty)$ against 't' and M_t/M_∞ against $t^{1/2}$. Notably, the graph of $\ln(1 - M_t/M_\infty)$ against time displays linearity when $M_t/M_\infty > 0.5$. This linearity allows for accurately determining the diffusion coefficient by calculating the gradient, achieving a precision of 99% [166]. It's essential to acknowledge the potential impact of extra crystalline resistance, which can decelerate the initial adsorption rate and disrupt the linearity observed in the M_t/M_∞ against the time graph. Furthermore, a significant variation in crystallite size can also interfere with the linearity observed in the $\ln(1 - M_t/M_\infty)$ versus time graph. Additionally, it's crucial to recognize that the solution provided by Eq. (11) assumes isothermal behavior. However, it's important to note that isothermal conditions may not always be maintained, especially during rapid adsorption [166].

3.2.2 Linear Driving Force (LDF)

The LDF (Linear Driving Force) Model describes how adsorbate concentration on a per-mass unit basis within a solid adsorbent evolves over time. This change is determined by the adsorbate concentration within the adsorbent, the concentration in the gas phase, and the kinetic coefficient governing the diffusion process. When the diffusion process in the solid is the controlling stage, the adsorption kinetic is described by the following equation [167]:

$$\frac{dW}{dt} = k_L [W^* - W] \quad (13)$$

When the diffusion process in the gas phase around the solid particle (external mass transfer) is the controlling stage, LDF equation is:

$$\frac{dW}{dt} = \frac{k_f S_p (C - C_s)}{n_L} \quad (14)$$

where k_L = LDF mass transfer coefficient, W = Mean adsorbate loading at time t , W^* = Equilibrium adsorbate loading, k_f = External mass transfer coefficient, S_p = Particle surface, C = Adsorbate concentration in the gas external film around the particle, C_s = Concentration of the adsorbate in the particle surface. Due to its simplicity and accuracy, the LDF (Linear Driving Force) model is extensively employed in energy storage applications. The LDF method successfully simplifies the mass transfer resistance to a convenient form. Internal and exterior mass transfer resistance must be considered when simulating adsorption processes. Internal mass transfer resistance refers to adsorbate diffusion within the pores of the adsorbent material, whereas external mass transfer resistance refers to adsorbate transport between the bulk fluid and the adsorbent surface.

3.3 Gas dynamics in porous media

Two extensively used methods for determining adsorbate flow inside the bed are Darcy's law [168] and Ergun's equation [169]. Darcy's Law is a fundamental equation that describes the velocity field of fluids flowing through a porous medium. It accomplishes this by utilizing average flow variables measured over a unit volume. Darcy's Law describes how fluids move through porous materials by examining the flow properties averaged over a defined volume. This equation is a cornerstone in studying fluid dynamics in porous media, allowing us to understand and predict how fluids, including gases and liquids, move through these complex environments. The velocity field through a porous medium by using average flow variables over a unit volume can be presented as:

$$z = -\frac{\kappa}{\mu} \nabla p \quad (10)$$

where q is the Darcy velocity, κ is the hydraulic permeability of the porous material, and μ is the dynamic viscosity. Darcy's Law and the Continuity equation as Eq. (11), where ρ is the density of the fluid and ϵ is the porosity, can be formulated as:

$$\frac{\partial}{\partial t} (\rho\epsilon) + \nabla \cdot (\rho q) = 0 \quad (11)$$

This equation represents how fluid density and porosity relate to fluid flow and changes in density within a porous medium. It is a fundamental equation for studying fluid

dynamics in porous media, particularly when considering the transport of fluids such as gases and liquids through these materials. It assumes steady-state, incompressible flow in a homogeneous, isotropic medium with constant fluid properties. However, it's limited in non-Darcy flow, transient conditions, and complex pore-scale effects. Understanding these assumptions and limitations is crucial for applying Darcy's Law effectively in various practical scenarios.

Ergun's equation encompasses broader effects, accounting for viscous and inertial forces. In contrast, Darcy's law assumes that inertial forces are insignificant compared to viscous forces. Ergun's equation, used to estimate pressure drop in packed beds, operates under several key assumptions and limitations. It assumes either laminar or turbulent flow, excluding the transitional regime, and presupposes the presence of uniformly sized spherical particles evenly distributed without channeling. The equation also relies on the assumptions of steady-state, incompressible flow, and interstitial voids filled with the same fluid as the one flowing through the bed. Despite its empirical nature, Ergun's equation may not provide precise predictions for systems with non-spherical particles or irregular distributions, and it may not be suitable for extreme flow rates. Complex fluid-particle interactions, particle characteristics, and heat transfer are not considered, so users must be mindful of these constraints and may opt for more accurate methods, such as computational fluid dynamics or experimental data when facing fewer ideal scenarios.

In modeling packed beds under turbulent flows, two critical factors are considered: permeability and inertial loss coefficients. These coefficients help describe the pressure drop and flow behavior through the packed bed. One commonly employed technique to determine the appropriate constants for these coefficients involves using the Ergun equation, a semi-empirical correlation widely applicable over a broad range of Reynolds numbers and various types of packing materials [170]. The Ergun equation provides a helpful framework for estimating pressure drops in packed beds and can aid in characterizing and modeling turbulent flow within these systems.

$$\frac{|\Delta p|}{L} = \frac{150\mu (1 - \epsilon)^2}{D_p^2 \epsilon^3} v_\infty + \frac{1.75\rho (1 - \epsilon)^2}{D_p \epsilon^3} v_\infty^2 \quad (12)$$

When modeling laminar flow through a packed bed, it is expected to simplify the analysis by dropping the second term in the Ergun equation, representing the inertial loss. This simplification results in the Blake-Kozeny equation. The Blake-Kozeny equation is a modification of Ergun's equation tailored for laminar flow conditions and is particularly useful when the Reynolds number of

the flow is sufficiently low, such that inertial effects can be neglected. In this simplified form, the equation mainly focuses on the permeability and viscous losses within the packed bed and provides a more accurate representation of pressure drop in such laminar flow scenarios.

$$\frac{|\Delta p|}{L} = \frac{150\mu (1 - \epsilon)^2}{D_p^2 \epsilon^3} v_\infty \quad (13)$$

The use of Navier–Stokes (NS) equations to predict gas flow through porous materials is infrequent due to challenges associated with the unknown pore network and computational issues. Table 4 summarizes modeling efforts in the literature concerning solid–gas adsorption processes for heat storage and transformation. These studies are classified based on the adsorption pair modeled, the modeling purpose, parameterization, the approach to adsorption equilibria, and the models employed for internal and external mass transfer resistance. The review also contains the numerical methods and software for solving the model equations. Readers are urged to refer to the thorough research undertaken by Nagel et al. [161] for a complete and extensive assessment of numerical modeling in thermochemical heat storage and transformation processes.

4 Seasonal solar thermochemical energy storage

This solar thermal energy storage sorption system includes an adsorbent reactor and a refrigerant container, as shown in Fig. 4 [197]. The reactor features a shell-and-finned tube design, with the adsorbent compressed between the fins and a heat transfer fluid circulating in the tubes. Each finned tube functions as a module, enabling easy scalability by adding or removing modules. The system is optimized for efficient solar thermal energy recovery from flat-plate and evacuated tube solar collectors due to its choice of materials with low desorption temperatures. However, thermal charging depends on the adsorbent temperature surpassing the desorption equilibrium temperature, which is dictated by the refrigerant condensation pressure and is influenced by varying weather conditions. Hot water temperatures for space heating are predefined based on end-user needs. While the system aims to cover winter heating demand, its success depends on practical operating conditions and fluctuating ambient temperatures. Ma et al. [197] assessed the viability of a seasonal solar thermal energy storage (SSTES) system utilizing ammonia-based chemisorption for residential use in the UK. The dynamic charging and discharging performance of the SSTES was simulated using actual weather data, solar thermal collector models, domestic heating demand models, and chemisorption models.

Table 4 Summary of modeling techniques

| Working pairs | Isotherm equation | Kinetics | Mass transport equation | Numerical model | Software | References |
|------------------------------|-------------------------------|----------|-------------------------|-----------------|---------------------|------------|
| Silica gel/ H ₂ O | Modified DA | LDF | Ergun | FDM | MATLAB | [171] |
| Silica gel/ H ₂ O | Tóth | LDF | - | FDM | - | [165] |
| silica gel/ H ₂ O | Empirical | LDF | Ergun | FVM | - | [39] |
| Silica gel/ H ₂ O | Freundlich | LDF | - | FDM | - | [172] |
| Silica gel/ H ₂ O | Empirical | LDF | Darcy's law | FVM | - | [173] |
| Silica gel/ H ₂ O | Tóth | - | - | FVM | Ansys Fluent | [36] |
| Silica gel/ H ₂ O | Tóth | LDF | - | - | MATLAB | [174, 175] |
| Silica gel/ H ₂ O | Empirical | LDF | - | FDM | - | [176] |
| Silica gel/ H ₂ O | Tóth isoth | - | - | FDM | - | [177] |
| Silica gel/ H ₂ O | Modified DA | - | - | FDM | MATLAB | [178] |
| Silica gel/ H ₂ O | Empirical | NS | - | FEM | COMSOL Multiphysics | [179] |
| Silica gel/ H ₂ O | Empirical | LDF | - | FDM | - | [38] |
| Silica gel/ H ₂ O | Empirical | LDF | Darcy's law | FDM | - | [180] |
| Silica gel/ H ₂ O | Tóth | LDF | Darcy's law | FVM | Ansys Fluent | [33] |
| Silica gel/ H ₂ O | Modified DR | derived | derived | FDM | - | [181] |
| Zeolite/ H ₂ O | DA | LDF | Brinkman | FEM | COMSOL Multiphysics | [54] |
| Zeolite/ H ₂ O | Langmuir | - | Ergun | FDM | - | [182] |
| Zeolite/ H ₂ O | DR | LDF | - | FEM | COMSOL Multiphysics | [183–185] |
| Zeolite/ H ₂ O | DP theory, Núñez modification | LDF | - | - | Modelica | [51] |
| Zeolite/ H ₂ O | Empirical | LDF | Darcy's law | FVM | Dymola | [186] |
| Zeolite/ H ₂ O | Modified DA | LDF | - | FVM | - | [187] |
| Zeolite/ H ₂ O | Gorbach model | - | - | - | PDEX, TRNSYS | [188] |
| Zeolite/ H ₂ O | Empirical | - | Ergun | FVM | - | [189] |
| Zeolite/ H ₂ O | Empirical | LDF | Darcy's law | FDM | Dymola | [190] |
| Zeolite/ H ₂ O | Empirical | - | Darcy's law | FDM | - | [191, 192] |
| Zeolite/ H ₂ O | Modified Langmuir | LDF | Poiseuille, | FVM | - | [52] |
| Zeolite/ H ₂ O | Empirical | - | Ergun | FDM | - | [193] |
| Zeolite/ H ₂ O | Modified DA | LDF | Darcy's law | FDM | - | [194] |
| Zeolite/ H ₂ O | - | NS | NS | FDM | - | [195] |
| Zeolite/ H ₂ O | DA | LDF | Brinkman | - | - | [53] |
| Zeolite/ H ₂ O | DR | NS | Darcy's law | FVM | - | [196] |
| Zeolite/ H ₂ O | DP theory, Núñez | - | - | - | OpenGeoSys | [50, 160] |

The choice of working salts was critical in system design and dynamic performance. The CaCl₂-4/8NH₃ chemisorption system could meet nearly 100% of space heating demand when using low-temperature heating facilities during the discharging phase. However, its relatively higher desorption temperature and the limited sunlight available in Newcastle-upon-Tyne led to the requirement for a larger solar collector area, often exceeding the available roof space of typical dwellings [197]. Conversely, the NaBr-0/5.25NH₃ chemisorption system could contribute only 18.6% of the heating demand because the discharged heat's temperature fell short of the required level for most heating seasons. The most promising scenario studied involved utilizing the

BaCl₂-0/8NH₃ chemisorption SSTES with a storage volume of 45.2 m³, low-temperature heating facilities, and a 30.5 m² solar collector. This configuration could cover approximately 57.4% of space heating for a dwelling with a heat loss coefficient of 150 W/K.

Effective space heating relies on meeting the discharged heat's quantity and quality requirements. Adjusting the storage capacity is achievable by modifying the number of solar collectors and the size of the storage system. However, a critical factor is the temperature of the incoming hot water. In the face of fluctuating ambient temperatures during the heating season, there's a risk that even with a fully charged SSTES, it may fall short of covering 100% of the heating demand. This can happen

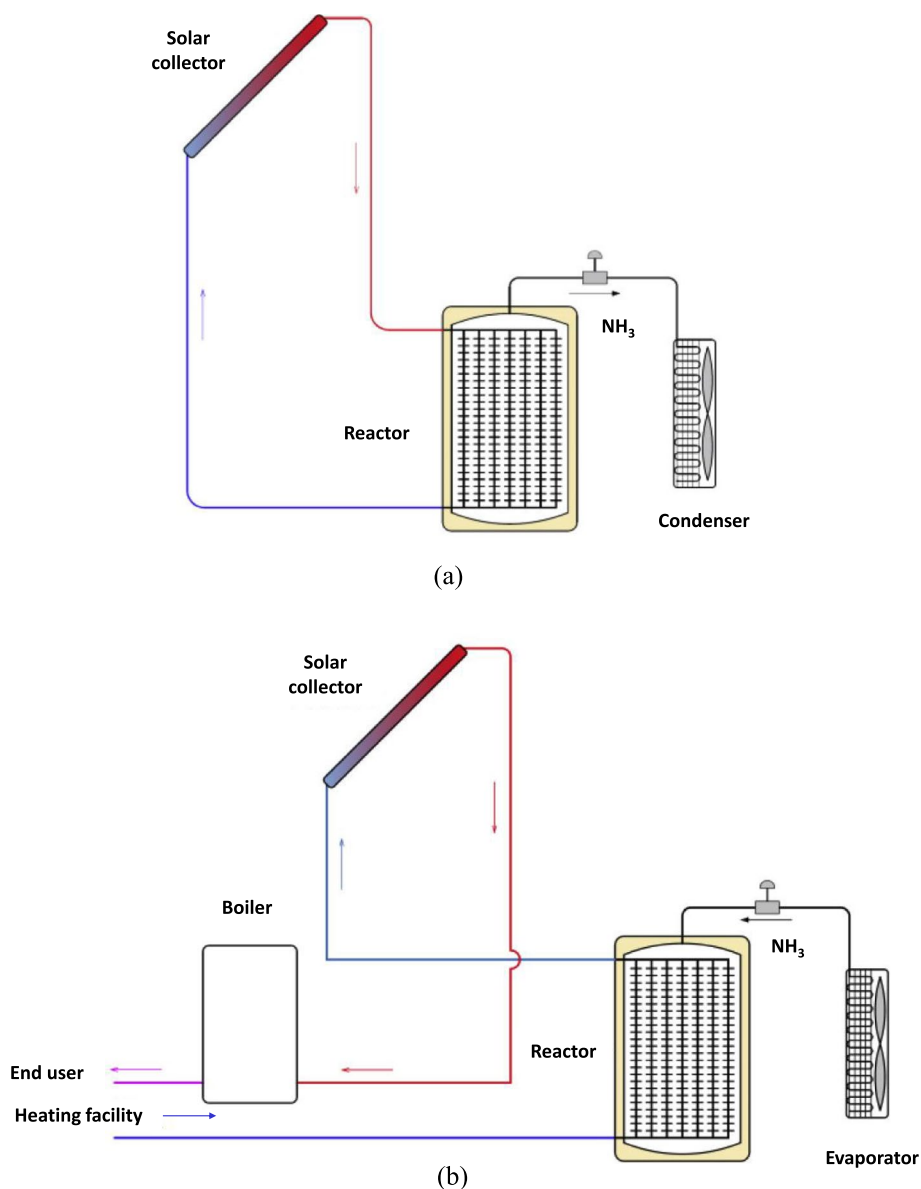


Fig. 4 Closed cycle adsorption system (a) charging (b) discharging [197]

when the adsorption equilibrium temperature isn't adequate to heat the return water to the desired feed water temperature. In more challenging situations, the adsorption temperature might even be lower than the return water temperature, as shown in Fig. 5. To address this challenge, a reevaluation of the choice of working salts is necessary. The equilibrium line for the preferred salt-ammonia reaction in SSTES applications should have a gentler slope on the Clausius-Clapeyron pressure-temperature diagram. Such a design allows the working salt to possess a relatively low desorption temperature, ensuring high thermal efficiency of solar collectors in summer

while still achieving sufficiently high adsorption temperatures in winter to meet space heating requirements.

Yue et al. [198] present a solar heating system incorporating seasonal and cascade thermal-energy storage using a zeolite-water pair. This innovative design not only boosts system efficiency through cascade storage but also maximizes the effective utilization of solar energy. Furthermore, they achieve a higher energy storage density by integrating daily and cross-seasonal energy storage. A mathematical model was developed to analyze the system's performance. The study evaluates the system's performance in heating and non-heating seasons, with

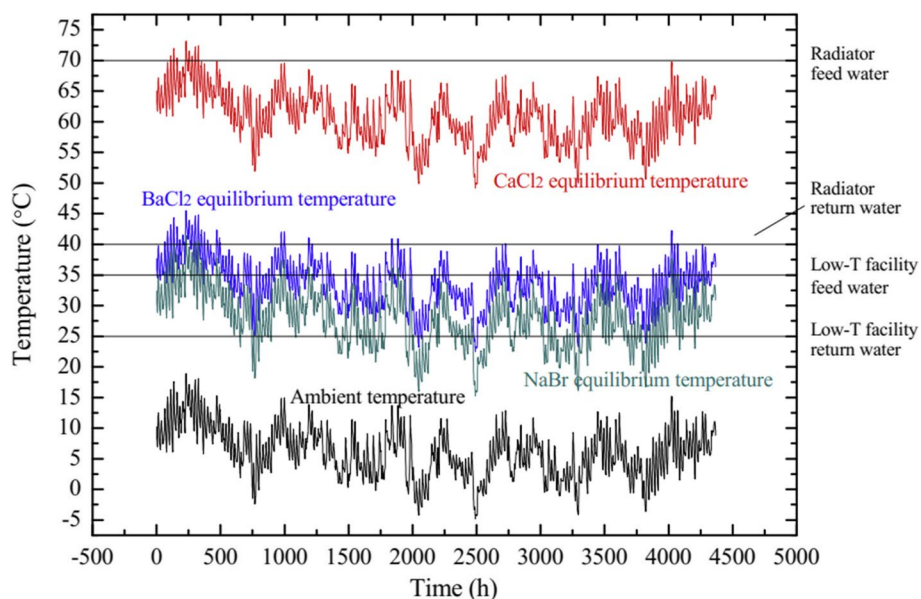


Fig. 5 Ambient Temperature and Chemisorption Equilibrium Temperature Under 1.0 Bar Equilibrium Pressure Drop During Thermal Discharging Stage [197]

Chifeng City, China, as a practical case study. The findings demonstrate that the proposed system outperforms the reference system, achieving a 2.88% higher average collection efficiency during non-heating seasons and a 7.4% improvement in the heating season. Additionally, the utilization efficiency of the proposed system reaches 37.16%, surpassing the reference system by 3.26%. Moreover, the system generates 9.66% more heat supply, totaling 2135 GJ during the heating season. This research presents an efficient solution for large-scale space heating applications that rely on solar energy.

Crespo et al. [199] studied a solar-driven water-based sorption system (Fig. 6) for seasonal energy storage evaluated in three European cities: Paris, Munich, and Stockholm. With 17.5 m² of solar collectors and 3.6 m³ of storage, the system achieved solar fractions between 28 and 45%, providing domestic hot water and space heating to a single-family house. The system's coefficient of performance (COP) ranged from 0.27 to 0.31, with Stockholm performing best due to optimal control and high charging efficiency. However, only 76% of the storage capacity was used in winter due to limited solar heat. Optimal control identified the minimum storage size to reduce costs, and none of the locations fully utilized the system's capacity. The system was independent of ambient temperature during winter, operating in very low temperatures, except in Paris, where ambient air was used for discharge due to milder winters. In summary, this sorption storage system can work well in European climates with intelligent control adaptation to local

conditions, offering an efficient way to store and use solar energy for heating.

The discharging efficiency of the seasonal sorption systems in the three different climatic zones exhibited similar overall performance. However, their winter operation varied significantly due to diverse weather conditions, as shown in Fig. 7. In Paris, the sorption thermal energy storage (TES) required approximately six months to achieve complete discharge, with the fastest discharges occurring during periods of low space heating (SH) demand, benefiting from ambient heat. In Munich, the sorption TES was fully discharged in about four months, driven by higher solar irradiation availability and increased thermal demand during the colder season. Stockholm saw around 72% of its stored energy released in 4.5 months, with intermittent discharging due to periods of high SH demand but low solar irradiation. These differences highlight the local climate's influence on these systems' operational dynamics.

Jiang et al. [200] investigated a novel hybrid sorption thermal energy storage (TES) system designed to harness ultra-low-grade solar heat, focusing on addressing winter heating needs in cold regions. By integrating this system with a water-based solar photovoltaic-thermal (PVT) setup, the study observed notable improvements in energy efficiency (0.52 to 0.57) and overall exergy efficiency (0.059 to 0.062) as water temperatures increased from 31.4 °C to 51.2 °C in Hangzhou. Notably, in Helsinki, the overall exergy efficiency reached 0.55, representing a 4.3% increase compared to Hangzhou. This

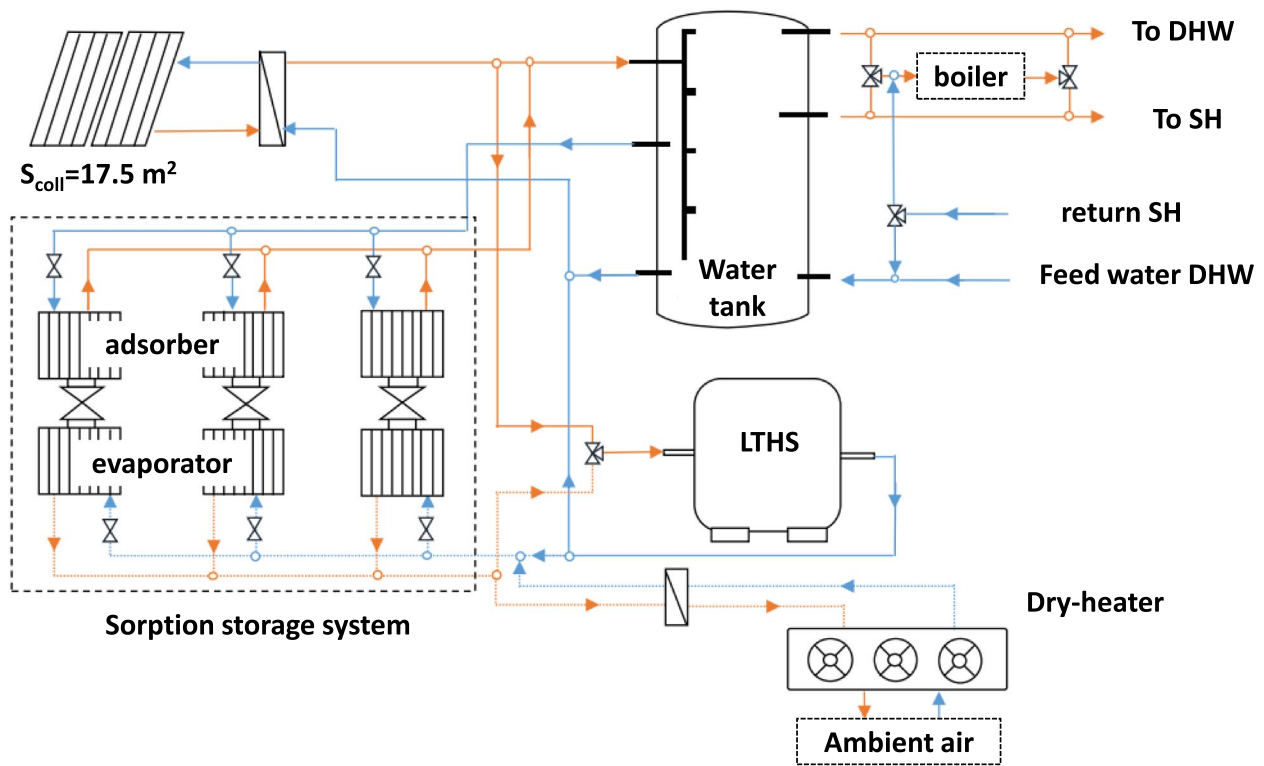


Fig. 6 System for winter configuration [199]

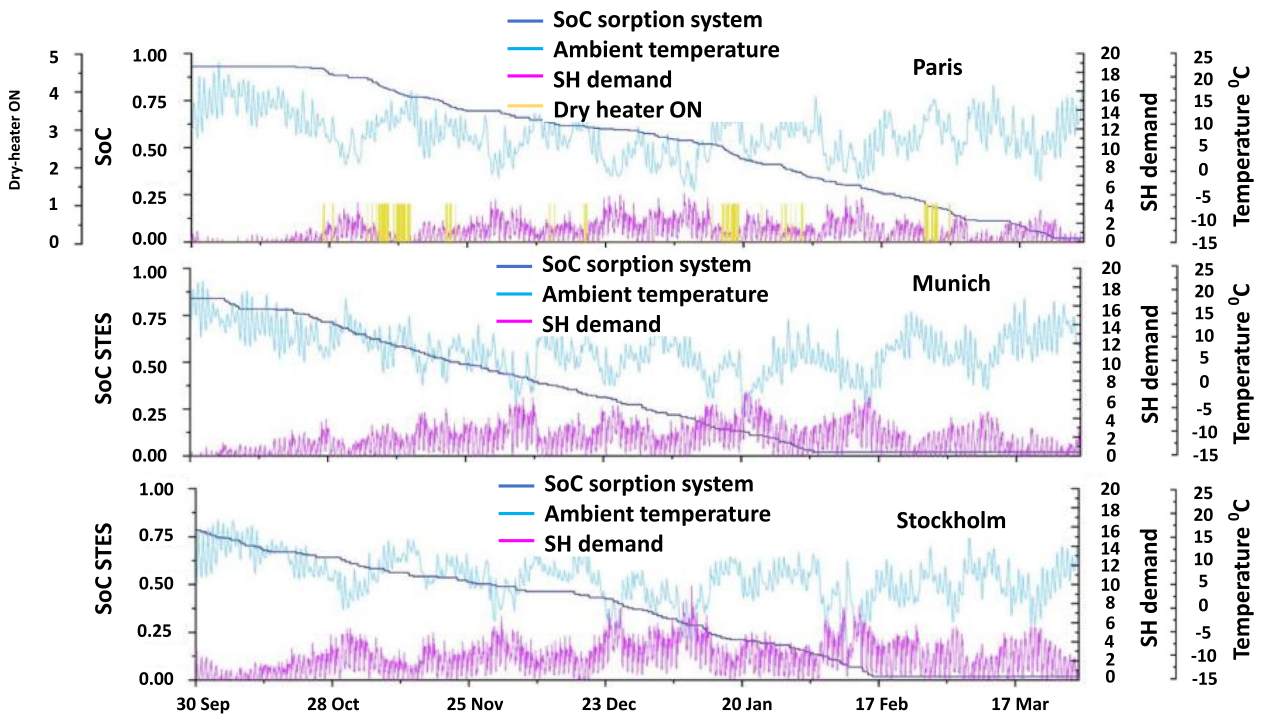


Fig. 7 Variables of Paris, Munich, and Stockholm during winter (from October to March) [199]

research highlights the promising potential of the hybrid TES-PVT system for severe cold regions.

Figure 8 [200] presents a schematic depiction of the hybrid thermochemical sorption thermal energy storage (TES) system tailored for harnessing ultra-low temperature solar energy. During the summer charging, this system utilizes solar photovoltaic-thermal (PVT) systems

or waste heat sources as the primary heat input. When the temperature surpasses 50 °C, supplementary thermal techniques, like sorption refrigeration, come into play to bring down the heat source temperature. The hybrid TES system consists of essential components, including a sorption reactor, condenser, evaporator, compressor, and valves, serving as the secondary stage to recover

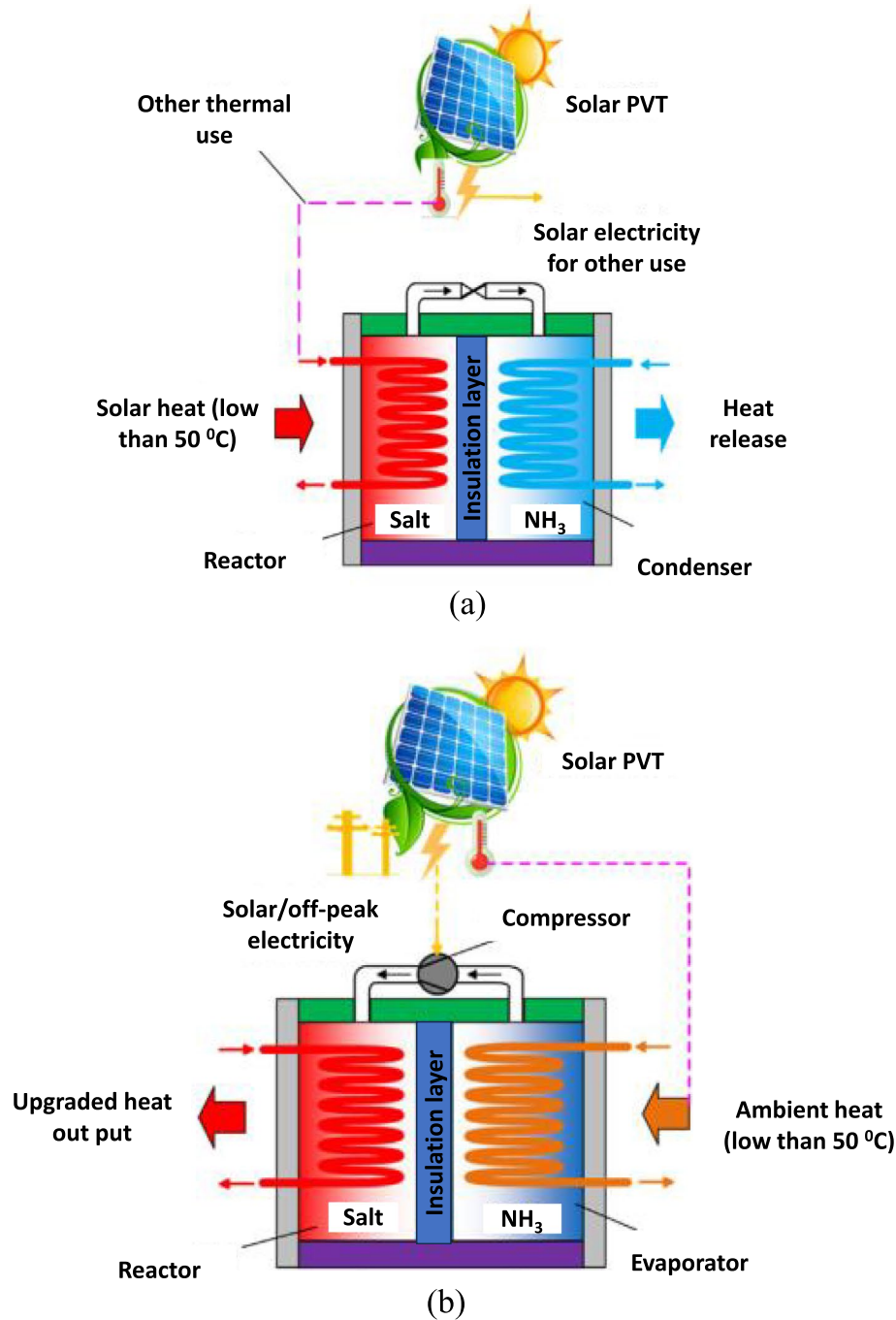


Fig. 8 Hybrid thermochemical sorption TES system for solar utilization (a) charging phase in summer; (b) discharging phase in winter [200]

heat below the 50 °C threshold. This recovered heat powers the desorption process of ammonia from the sorption reactor, with the released heat dissipating into the environment.

The process stores and converts thermal energy from the PVT system into the chemical potential of the sorption working pair. In the winter discharging process, where the PVT system’s heat output is relatively low for direct heating, ultra-low heat is harnessed to facilitate ammonia evaporation. The compressor, powered by electricity from the PVT system or off-peak grid, pressurizes

the ammonia for sorption in the reactor, effectively elevating the heat to meet winter heating requirements.

Adjusting the collector-tank ratio in a PVT system allows for fine-tuning final water temperatures and energy output levels, as demonstrated in Fig. 9 for a collector-tank ratio of 0.02. Notably, to account for the limitation of hourly weather data from the EnergyPlus Weather Data website, we applied linear interpolation to obtain ambient temperature and solar irradiance values at a 10-s interval, matching the simulation model’s time step. Initially, the PVT system exhibits low thermal

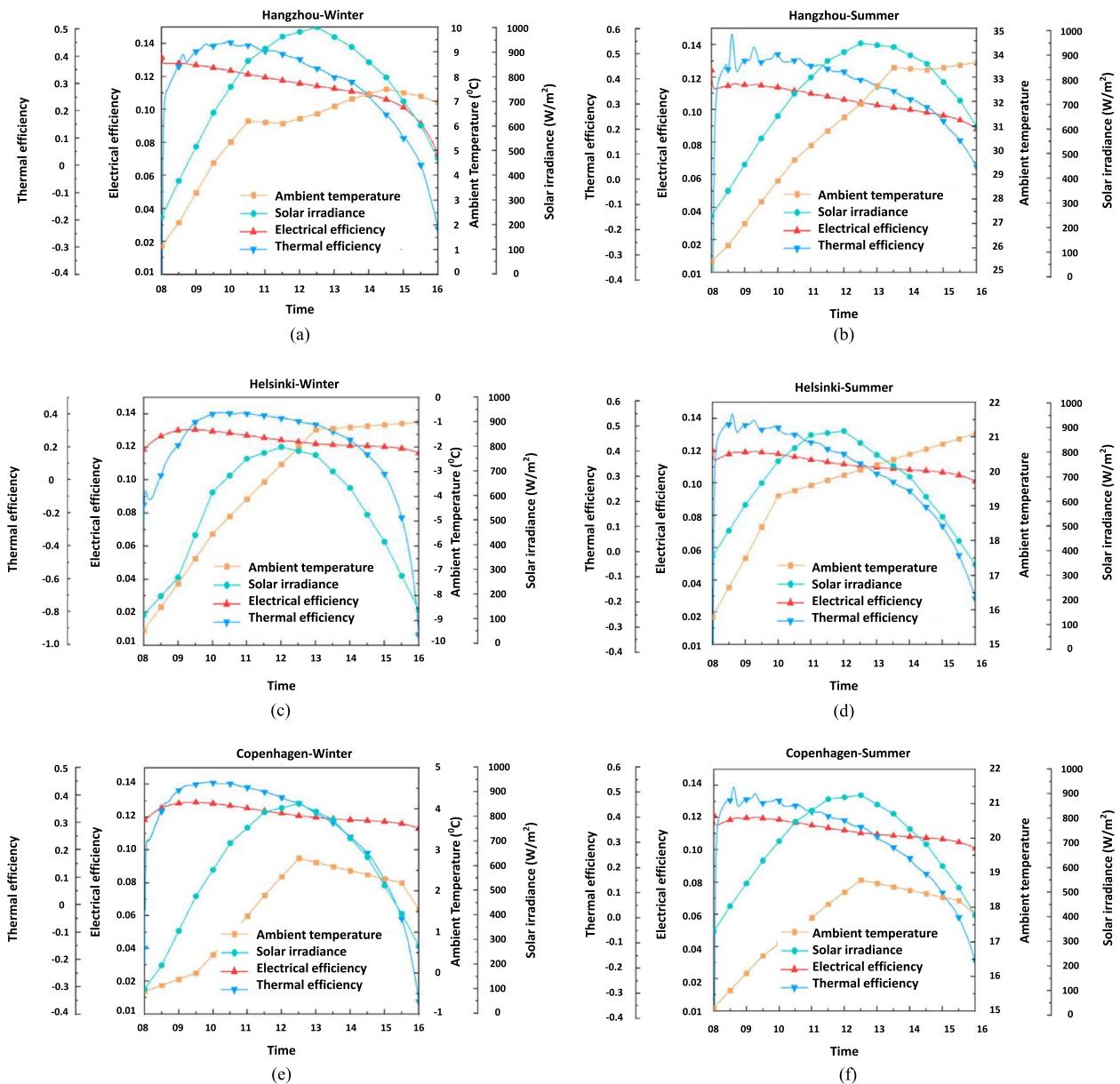


Fig. 9 Ambient temperature and solar irradiance on the selected days and the corresponding transient electrical and thermal performance of the PVT system with a collector-tank ratio of 0.02 [200]

efficiency due to the cold starting temperatures of its components. However, within just under 20 steps, the efficiency sharply rises to a reasonable level as the system nears its quasi-steady state. Towards the end of the simulation, thermal efficiency drops, sometimes even becoming negative, primarily due to significant heat loss and reduced solar irradiance.

Sorption-based solar thermal energy storage systems offer promise for meeting space heating needs, but their efficiency depends on factors like working materials selection, system design, and local climate conditions. These systems utilize chemisorption and sorption reactions to store and release thermal energy efficiently, and they can potentially cover a substantial portion of heating needs. Challenges arise from fluctuating ambient temperatures, affecting the ability to achieve complete heating coverage. Careful consideration of adsorption equilibrium temperature and material selection is necessary. Innovative methods like cascade thermal energy and cross-seasonal energy storage have improved efficiency and heating supply, offering solutions for large-scale heating needs. Integrating sorption thermal energy storage with solar photovoltaic-thermal technology, hybrid systems offer the potential for recovering ultra-low-grade solar heat, especially in cold regions, providing a holistic approach to winter heating requirements.

5 Conclusions

This study comprehensively looks at thermochemical materials (TCMs) used for heat storage in solar energy systems for buildings. The study focuses on TCMs with charging temperatures less than 140 °C and addresses the models used to forecast and optimize the performance of thermochemical storage systems. Examining working pairs for thermochemical heat storage found a few drawbacks, including high charging temperature, poor energy density, corrosiveness, thermal/chemical instability, ecologically unfriendly manufacture, and high cost. However, sorption materials incorporating water vapor as sorbate, notably zeolites and their composites with hygroscopic inorganic salt hydrates and microporous aluminophosphates, show exciting properties. Nonetheless, there is a difference in the energy storage density of these materials at the material level and within the entire system. To characterize adsorption equilibria, numerical modeling approaches in solid–gas adsorption processes primarily depend on the Dubinin–Polanyi theory, Darcy’s law, and the LDF model to estimate pressure gradient and adsorption rate. More study is needed to improve our understanding of the interrelationship between material synthesis, structural qualities, and system-level attributes to promote the development of thermochemical heat storage systems. This understanding will be essential in

developing more efficient and effective thermochemical heat storage technologies .

Acknowledgements

This research was supported by Basic Science Research Program through the National Research Foundation of Korea (NRF) funded by the Ministry of Education (No. 2017R1D1A1B05030422)

Authors’ contributions

Abdullah: investigation, writing-original draft. M. Koushaeian: review and editing, investigation. N. A. Shah: Writing-review, supervision. J. D. Chung: Supervision, project administration.

Availability of data and materials

Data pertaining to this study can be obtained from the corresponding author upon a reasonable request.

Declarations

Competing interests

The authors declare that they have no competing interests.

Received: 25 May 2023 Accepted: 20 November 2023

Published online: 02 January 2024

References

1. V. Gaigbe-Togbe, L. Bassarsky, D. Gu, T. Spoorenberg, and L. Zeifman, World Population Prospects 2022. 2022. Available: https://www.un.org/development/desa/pd/sites/www.un.org.development.desa.pd/files/wpp2022_summary_of_results.pdf
2. “IEA(2022).Heating,IEA,Paris,” 2022. <https://www.iea.org/reports/heating>
3. Hickel, R. (1955). Contribution à l’exploration radiologique des vertèbres lombaires agrandies et des quatre derniers interlignes vertébraux sur un seul film. *Presse Medicale (Paris, France: 1983)*, 63(30), 619.
4. “Reforming Korea’s Electricity Market for Net Zero,” *Reforming Korea’s Electr. Mark. Net Zero*, no. December, 2022, doi: <https://doi.org/10.1787/47d4e925-en>.
5. Sunku Prasad, J., Muthukumar, P., Desai, F., Basu, D. N., & Rahman, M. M. (2019). A critical review of high-temperature reversible thermochemical energy storage systems. *Appl Energy*, 254, 113733.
6. Mahon, H., O’Connor, D., Friedrich, D., & Hughes, B. (2022). A review of thermal energy storage technologies for seasonal loops. *Energy*, 239, 122207. <https://doi.org/10.1016/j.energy.2021.122207>
7. D. Sonar, “Chapter 4 - Renewable energy based trigeneration systems—technologies, challenges and opportunities,” in *Renewable-Energy-Driven Future*, J. Ren, Ed. Academic Press, 2021, pp. 125–168. doi: <https://doi.org/10.1016/B978-0-12-820539-6.00004-2>.
8. Tatsidjodoung, P., Le Pierrès, N., & Luo, L. (2013). A review of potential materials for thermal energy storage in building applications. *Renew Sust Energy Rev*, 18, 327–349. <https://doi.org/10.1016/j.rser.2012.10.025>
9. Harald Mehling, L. F. C. (2008). *Heat and cold storage with PCM* (1st ed.). Heidelberg: Springer Berlin.
10. N’Tsoukpoe, K. E., Liu, H., Le Pierrès, N., & Luo, L. (2009). A review on long-term sorption solar energy storage. *Renew Sust Energy Rev*, 13(9), 2385–2396. <https://doi.org/10.1016/j.rser.2009.05.008>
11. Abedin, A. H. (2011). A critical review of thermochemical energy storage systems. *Open Renew Energy J*, 4(1), 42–46. <https://doi.org/10.2174/1876387101004010042>
12. Kalaiselvam, R. P. S. (2014). Thermal energy storage technologies for sustainability systems design, assessment and applications. *Elsevier*. <https://doi.org/10.1016/C2013-0-09744-7>
13. McGlashan, M. L. (1970). No title. *Pure Appl Chem*, 21(1), 1–44. <https://doi.org/10.1351/pac197021010001>
14. J. C. Hadorn, “Advanced Storage Concepts for Active Solar Energy,” *EUROSUN 2008; 1st Int. Congr. heating, Cool. Build.*, pp. 2085–2092, 2008. Available: <http://www.iea-shc.org/>.

15. J. H. Davidson, J. Quinnell, J. Burch, H. a Zondag, R. De Boer, C. Finck, R. Cuypers, L. F. Cabeza, A. Heinz, D. Jahnig, S. Furbo, and F. Bertsch, "Development of Space Heating and Domestic Hot Water Systems with Compact Thermal Energy Storage," *Compact Therm. Energy Storage Mater. Dev. Syst. Integr.*, no. July, 2013. Available: <http://www.iea-shc.org/task42>. Accessed April 2015.
16. N'Tsoukpo, K. E., Restuccia, G., Schmidt, T., & Py, X. (2014). The size of sorbents in low pressure sorption or thermochemical energy storage processes. *Energy*, 77, 983–998. <https://doi.org/10.1016/j.energy.2014.10.013>
17. Scapino, L., Zondag, H. A., Van Bael, J., Diriken, J., & Rindt, C. C. M. (2017). Sorption heat storage for long-term low-temperature applications: a review on the advancements at material and prototype scale. *Appl Energy*, 190, 920–948. <https://doi.org/10.1016/j.apenergy.2016.12.148>
18. FopahLele, A., N'Tsoukpo, K. E., Osterland, T., Kuznik, F., & Ruck, W. K. L. (2015). Thermal conductivity measurement of thermochemical storage materials. *Appl Therm Eng*, 89, 926.
19. Aydin, D., Casey, S. P., & Riffat, S. (2015). The latest advancements on thermochemical heat storage systems. *Renew Sust Energy Rev*, 41, 356–367. <https://doi.org/10.1016/j.rser.2014.08.054>
20. C. Bales, "Thermal Properties of Materials for Thermo-chemical Storage of Solar Heat," IEA SHC - Task 32 - Advanced storage concepts Sol. low energy Build., p. 20, 2005.
21. Lefebvre, D., & Tezel, F. H. (2017). A review of energy storage technologies with a focus on adsorption thermal energy storage processes for heating applications. *Renew Sust Energy Rev*, 67, 116–125. <https://doi.org/10.1016/j.rser.2016.08.019>
22. Ayaz, H., Chinnasamy, V., Yong, J., & Cho, H. (2021). Review of technologies and recent advances in low-temperature sorption thermal storage systems. *Energies*, 14(19), 1–36. <https://doi.org/10.3390/en14196052>
23. J. Hadorn, IEA SHC Task32 - Thermal energy storage Handbook - Digital version - June 2005 - Hadorn editor - 179 pages ISBN 84–8409–877-X, no. June 2005. 2020.
24. C. Bales, P. Gantenbein, D. Jaenig, H. Kerskes, K. Summer, M. Van Essen, and R. Weber, "Laboratory Tests of Chemical Reactions and Prototype Sorption Storage Units," A Rep. IEA Sol. Heat. Cool. Program. - Task 32 Adv. storage concepts Sol. low energy Build., p. 55p., 2008.
25. W. Wagner, D. Jahnig, C. Isaksson, and R. Hausner, "Modularer Energiespeicher nach dem Sorptionsprinzip mit hoher Energiedichte (MODESTORE)," *Berichte aus Energie- und Umweltforsch.*, 2006.
26. Li, G., Qian, S., Lee, H., Hwang, Y., & Radermacher, R. (2014). Experimental investigation of energy and exergy performance of short term adsorption heat storage for residential application. *Energy*, 65, 675–691. <https://doi.org/10.1016/j.energy.2013.12.017>
27. Deshmukh, H., Maiya, M. P., & Srinivasa Murthy, S. (2017). Study of sorption based energy storage system with silica gel for heating application. *Appl Therm Eng*, 111, 1640–1646. <https://doi.org/10.1016/j.applthermaleng.2016.07.069>
28. Gartler, G., Jahnig, D., Purkarthofer, G., & Wagner, W. (2004). Development of a high energy density sorption storage system. *Eurosun*, 2004, 10.
29. Paksoy H. Thermal Energy Storage for Sustainable Energy Consumption NATO Science Series.
30. D. Jahnig, R. Hausner, W. Wagner, and C. Isaksson, "Thermo-chemical storage for solar space heating in a single-family house," AEE – INTEC (Austria), Ecostock Conf. New Jersey; 31 May - 02 June, pp. 1–7, 2006.
31. D. Basciotti and O. Pol, "a Theoretical Study of the Impact of Using Small Scale Thermo Chemical Storage Units in District Heating Networks," *Int. Sustain. Energy Conf.*, pp. 1–10, 2011.
32. Stritih, U., & Bombac, A. (2014). Description and analysis of adsorption heat storage device. *Stroj Vestnik/Journal Mech Eng*, 60(10), 619–628. <https://doi.org/10.5545/sv-jme.2014.1814>
33. Mitra, S., Aswin, N., & Dutta, P. (2016). Scaling analysis and numerical studies on water vapour adsorption in a columnar porous silica gel bed. *Int J Heat Mass Transfer*, 95, 853–864. <https://doi.org/10.1016/j.jijheatmasstransfer.2015.12.011>
34. Chua, H., Ng, K. C., Chakraborty, A., Oo, N. M., & Othman, M. A. (2002). Adsorption characteristics of silica gel + water systems. *J Chem Eng Data*, 47, 1177–1181. <https://doi.org/10.1021/je0255067>
35. Wang, X., Zimmermann, W., Ng, K. C., Chakraborty, A., & Keller, J. U. (2004). Investigation on the isotherm of silica gel+water systems. *Journal of Thermal Analysis and Calorimetry*, 76(2), 659–669. <https://doi.org/10.1023/B:JTAN.0000028045.96239.7e>
36. Aristov, Y. I., Tokarev, M. M., Freni, A., Glaznev, I. S., & Restuccia, G. (2006). Kinetics of water adsorption on silica Fuji Davison RD. *Microporous and Mesoporous Materials*, 96(1–3), 65–71. <https://doi.org/10.1016/j.micro-meso.2006.06.008>
37. Mitra, S., Oh, S. T., Saha, B. B., Dutta, P., & Srinivasan, K. (2015). Simulation study of the adsorption dynamics of cylindrical silica gel particles. *Heat Transf Res*, 46(2), 123–140. <https://doi.org/10.1615/HeatTransRes.2014007318>
38. Ilic, G. G., Mobedi, M., & Ullku, S. (2011). A dimensionless analysis of heat and mass transport in an adsorber with thin fins; uniform pressure approach. *Int Commun Heat Mass Transf*, 38(6), 790–797. <https://doi.org/10.1016/j.icheatmasstransfer.2011.03.001>
39. Niazmand, H., & Dabzadeh, I. (2012). Numerical simulation of heat and mass transfer in adsorbent beds with annular fins. *International Journal of Refrigeration*, 35(3), 581–593. <https://doi.org/10.1016/j.jrefrig.2011.05.013>
40. Bjurström, H., Karawacki, E., & Carlsson, B. (1984). Thermal conductivity of a microporous particulate medium. *International Journal of Heat and Mass Transfer*, 27(11), 2025–2036. [https://doi.org/10.1016/0017-9310\(84\)90189-3](https://doi.org/10.1016/0017-9310(84)90189-3)
41. Lu, Y. Z., Wang, R. Z., Zhang, M., & Jiangzhou, S. (2003). Adsorption cold storage system with zeolite–water working pair used for locomotive air conditioning. *Energy Convers. Manag.*, 44(10), 1733–1743. [https://doi.org/10.1016/S0196-8904\(02\)00169-3](https://doi.org/10.1016/S0196-8904(02)00169-3)
42. Bales C, Gantenbein P. "Laboratory prototypes of thermo-chemical and sorption storage units, Report B3—IEA SHC Task 32," Rep. B3—IEA SHC Task 32, 2007.
43. Abu-heiba A, Malhotra M, Gluesenkamp KR, Patel VK. Domestic Dish-washer Simulated Energy Efficiency Evaluation Using Thermoelectric Heat Pump for Water Heating and Dish Drying. pp. 1–11, 2018.
44. Jänchen, J., Ackermann, D., Weiler, E., Stach, H., & Brösicke, W. (2005). Calorimetric investigation on zeolites, AlPO₄'s and CaCl₂ impregnated attapulgite for thermochemical storage of heat. *Thermochemica Acta*, 434(1), 37–41. <https://doi.org/10.1016/j.tca.2005.01.009>
45. Weber, R., Asenbeck, S., Kerskes, H., & Drück, H. (2016). SolSpaces – testing and performance analysis of a segmented sorption store for solar thermal space heating. *Energy Procedia*, 91(C), 250–258. <https://doi.org/10.1016/j.egypro.2016.06.214>
46. B. Mette, H. Kerskes, H. Drück, T. Badenhop, F. Salg, and R. Gläser, "Thermochemical energy storage as an element for the energy turnaround," 8th Int. Renew. Energy Storage Conf. Exhib. (IRES 2013), no. January, pp. 1–10, 2013.
47. Mette, B., Kerskes, H., Drück, H., & Müller-Steinhagen, H. (2014). Experimental and numerical investigations on the water vapor adsorption isotherms and kinetics of binderless zeolite 13X. *International Journal of Heat and Mass Transfer*, 71, 555–561. <https://doi.org/10.1016/j.jijheatmasstransfer.2013.12.061>
48. Hauer, A. (2007). Evaluation of adsorbent materials for heat pump and thermal energy storage applications in open systems. *Adsorption*, 13(3), 399–405. <https://doi.org/10.1007/s10450-007-9054-0>
49. Johannes, K., Kuznik, F., Hubert, J.-L., Durier, F., & Obrecht, C. (2015). Design and characterisation of a high powered energy dense zeolite thermal energy storage system for buildings. *Applied Energy*, 159(C), 80–86. <https://doi.org/10.1016/j.apenergy.2015.0>
50. Lehmann, C., Beckert, S., Gläser, R., Kolditz, O., & Nagel, T. (2017). Assessment of adsorbate density models for numerical simulations of zeolite-based heat storage applications. *Applied Energy*, 185(P2), 1965–1970. <https://doi.org/10.1016/j.apenergy.2015.1>
51. Schreiber, H., Graf, S., Lanzerath, F., & Bardow, A. (2015). Adsorption thermal energy storage for cogeneration in industrial batch processes: experiment, dynamic modeling and system analysis. *Applied Thermal Engineering*, 89, 485–493. <https://doi.org/10.1016/j.applthermaleng.2015.06.016>
52. Leong, K. C., & Liu, Y. (2004). Numerical modeling of combined heat and mass transfer in the adsorbent bed of a zeolite/water cooling system. *Applied Thermal Engineering*, 24(16), 2359–2374. <https://doi.org/10.1016/j.applthermaleng.2004.02.014>
53. Pal, S., Hajj, M. R., Wong, W. P., & Puri, I. K. (2014). Thermal energy storage in porous materials with adsorption and desorption of moisture.

- International Journal of Heat and Mass Transfer*, 69, 285–292. <https://doi.org/10.1016/j.ijheatmasstransfer.2013.10.023>
54. Mette, B., Kerskes, H., & Drück, H. (2014). Experimental and numerical investigations of different reactor concepts for thermochemical energy storage. *Energy Procedia*, 57, 2380–2389. <https://doi.org/10.1016/j.egypro.2014.10.246>
 55. Jänchen, J., Ackermann, D., Stach, H., & Brösicke, W. (2004). Studies of the water adsorption on Zeolites and modified mesoporous materials for seasonal storage of solar heat. *Solar Energy*, 76(1), 339–344. <https://doi.org/10.1016/j.solener.2003.07.036>
 56. Hauer, A. (2002). Thermal energy storage with zeolite for heating and cooling applications. *Int Sorption Heat Pump Conf*, 1, 385–390.
 57. S. Hongois, F. Kuznik, P. Stevens, and J. Roux, Development and characterisation of a new MgSO₄-zeolite composite for long-term thermal energy storage To cite this version: HAL Id : hal-00683965. 2014.
 58. Zettl, B., Englmaier, G., & Steinmaurer, G. (2014). Development of a revolving drum reactor for open-sorption heat storage processes. *Applied Thermal Engineering*, 70, 42–49. <https://doi.org/10.1016/j.applthermaleng.2014.04.069>
 59. B. Michel, N. Mazet, S. Mauran, D. Stitou, J. Xu, B. Michel, N. Mazet, S. Mauran, D. Stitou, J. Xu, B. Michel, N. Mazet, S. Mauran, D. Stitou, and J. Xu, "Thermochemical process for seasonal storage of solar energy : characterization and modeling of a high-density reactive bed To cite this version: HAL Id : hal-00820757 Thermochemical process for seasonal storage of solar energy : characterization and mode," 2013.
 60. Kerskes H. Experimental and Numerical Investigations on Thermo Chemical Heat Storage. 2016:1–10. <https://doi.org/10.18086/eurosun.2010.16.14>.
 61. Kerskes, H., Heidemann, W., & Müller-Steinhagen, H. (2004). *Mono-Sorp - Ein weiterer Schritt auf dem Weg zur vollständig solarthermischen Gebäudeheizung*.
 62. Kerskes, H., Sommer, K., & Müller-Steinhagen, H. (2008). *MonoSorp - Ein integrales Konzept zur solarthermischen Gebäudeheizung mit Sorption-swärmspeicher* (pp. 55–59)
 63. Englmaier, G., Zettl, B., & Lager, D. (2014). *Characterisation of a Rotating Adsorber Designed for Thermochemical Heat Storage Processes*. <https://doi.org/10.18086/eurosun.2014.10.12>
 64. Cuypers, R., Maraz, N., Eversdijk, J., Finck, C., Henquet, E., Oversloot, H., Spijker, H., & Geus, A. (2012). Development of a seasonal thermochemical storage system. *Energy Procedia*, 30, 207–214. <https://doi.org/10.1016/j.egypro.2012.11.025>
 65. Finck, C., Spijker, H., Jong, A.-J., Henquet, E., Oversloot, H., & Cuypers, R. (2013). *Design of a modular 3 kWh thermochemical heat storage system for space heating application*.
 66. Finck, C., Henquet, E., van Soest, C., Oversloot, H., de Jong, A.-J., Cuypers, R., & van't Spijker, V. (2014). Experimental results of a 3 kWh thermochemical heat storage module for space heating application. *Energy Procedia*, 48, 320–326. <https://doi.org/10.1016/j.egypro.2014.02.037>
 67. Ristic A, Nataša Z, Zabukovec Logar N, Henninger S, Kaučič V. The performance of small-pore microporous aluminophosphates in low-temperature solar energy storage: the structure-property relationship. *Adv Funct Mater*. 2012;22. <https://doi.org/10.1002/adfm.201102734>.
 68. Henninger, S. K., Schmidt, F. P., & Henning, H.-M. (2010). Water adsorption characteristics of novel materials for heat transformation applications. *Applied Thermal Engineering*, 30(13), 1692–1702. <https://doi.org/10.1016/j.applthermaleng.2010.03.028>
 69. Van Essen, V. M., Cot Gores, J., Bleijendaal, L. P. J., Zondag, H. A., Schuitema, R., Bakker, M., & Van Helden, W. G. J. (2009). Characterization of salt hydrates for compact seasonal thermochemical storage. *Proc ASME 3rd Int Conf Energy Sustain 2009, ES2009*, 2, 825–830. <https://doi.org/10.1115/ES2009-90289>
 70. Hui, L., Edem, N. K., Nolwenn, L. P., & Lingai, L. (2011). Evaluation of a seasonal storage system of solar energy for house heating using different absorption couples. *Energy Convers Manag*, 52(6), 2427–2436. <https://doi.org/10.1016/j.enconman.2010.12.049>
 71. Quinnell, J. A., & Davidson, J. H. (2012). Mass transfer during sensible charging of a hybrid absorption/sensible storage tank. *Energy Procedia*, 30, 353–361. <https://doi.org/10.1016/j.egypro.2012.11.042>
 72. Rammelberg, H. U., Schmidt, T., & Ruck, W. (2012). Hydration and dehydration of salt hydrates and hydroxides for thermal energy storage - kinetics and energy release. *Energy Procedia*, 30, 362–369. <https://doi.org/10.1016/j.egypro.2012.11.043>
 73. Vasiliev, L. L., Mishkinis, D. A., Antukh, A. A., & Vasiliev, L. L. (2001). Solar-gas solid sorption refrigerator. *Adsorption*, 7(2), 149–161. <https://doi.org/10.1023/A:1011604326633>
 74. Quinnell, J. A., & Davidson, J. H. (2014). Heat and mass transfer during heating of a hybrid absorption/sensible storage tank. *Solar Energy*, 104, 19–28. <https://doi.org/10.1016/j.solener.2013.07.035>
 75. C. Bales, P. Gantenbein, D. Jaenig, H. Kerskes, M. van Essen, R. Weber, and H. Zondag, "Final Report of Subtask B 'Chemical and Sorption Storage' : Report B7 of Subtask B," p. 21, 2008. Available: <http://www.iea-shc.org/publications/downloads/task32-c7.pdf>.
 76. N'Tsoukpoe, K. E., Le Pierrès, N., & Luo, L. (2012). Numerical dynamic simulation and analysis of a lithium bromide/water long-term solar heat storage system. *Energy*, 37(1), 346–358. <https://doi.org/10.1016/j.egypro.2011.11.020>
 77. N'Tsoukpoe, K. E., Le Pierrès, N., & Luo, L. (2013). Experimentation of a LiBr–H₂O absorption process for long-term solar thermal storage: Prototype design and first results. *Energy*, 53, 179–198. <https://doi.org/10.1016/j.egypro.2013.02.023>
 78. B. Cerkvenik, P. Satzger, F. Ziegler, and A. Poredoš, "High efficient sorption cycles using CaO/H₂O and LiBr/H₂O for gas cooling," 1999, pp. RAES99–7603.pdf.
 79. N'Tsoukpoe, K. E., Le Pierrès, N., & Luo, L. (2012). Experimentation of a LiBr–H₂O absorption process for long term solar thermal storage. *Energy Procedia*, 30, 331–341. <https://doi.org/10.1016/j.egypro.2012.11.039>
 80. K. E. N, M. Perier-muzet, N. Le Pierrès, D. Mangin, K. E. N, M. Perier-muzet, N. Le Pierrès, L. Luo, and D. Mangin, "Thermodynamic study of a LiBr – H₂O absorption process for solar heat storage with crystallisation of the solution To cite this version : HAL Id : hal-01833509 Thermodynamic study of a LiBr – H₂O absorption process for solar heat storage with crystallisation," 2019.
 81. Weber, R., & Dorer, V. (2008). Long-term heat storage with NaOH. *Vacuum*, 82(7), 708–716. <https://doi.org/10.1016/j.vacuum.2007.10.018>
 82. Fumey, B., Weber, R., Gantenbein, P., Daguene-Frick, X., Williamson, T., & Dorer, V. (2014). Development of a closed sorption heat storage prototype. *Energy Procedia*, 46, 134–141. <https://doi.org/10.1016/j.egypro.2014.01.166>
 83. Fumey, B., Weber, R., Gantenbein, P., Daguene-Frick, X., Williamson, T., & Dorer, V. (2014). Closed sorption heat storage based on aqueous sodium hydroxide. *Energy Procedia*, 48, 337–346. <https://doi.org/10.1016/j.egypro.2014.02.039>
 84. Daguene-Frick, X., Gantenbein, P., Frank, E., Fumey, B., Weber, R., & Williamson, T. (2014). Reaction zone development for an aqueous sodium hydroxide seasonal thermal energy storage. *Energy Procedia*, 57, 2426–2435. <https://doi.org/10.1016/j.egypro.2014.10.251>
 85. Fumey, B., Weber, R., Gantenbein, P., Daguene-Frick, X., Williamson, T., Dorer, V., & Carmeliet, J. (2014). Experience on the development of a thermo-chemical storage system based on aqueous sodium hydroxide. *Energy Procedia*, 57, 2370–2379. <https://doi.org/10.1016/j.egypro.2014.10.245>
 86. Fumey, B., Weber, R., Gantenbein, P., Daguene-Frick, X., Stoller, S., Fricker, R., & Dorer, V. (2015). Operation results of a closed sorption heat storage prototype. *Energy Procedia*, 73, 324–330. <https://doi.org/10.1016/j.egypro.2015.07.698>
 87. Daguene-Frick, X., Gantenbein, P., Frank, E., Fumey, B., & Weber, R. (2015). Development of a numerical model for the reaction zone design of an aqueous sodium hydroxide seasonal thermal energy storage. *Solar Energy*, 121, 17–30. <https://doi.org/10.1016/j.solener.2015.06.009>
 88. Daguene-Frick, X., Gantenbein, P., Rommel, M., Fumey, B., Weber, R., Goonesekera, K., & Williamson, T. (2015). Seasonal solar thermal absorption energy storage development. *Chimia (Aarau)*, 69(12), 784–788. <https://doi.org/10.2533/chimia.2015.784>
 89. Michel, B., Mazet, N., Mauran, S., Stitou, D., & Xu, J. (2012). Thermochemical process for seasonal storage of solar energy: characterization and modeling of a high density reactive bed. *Energy*, 47(1), 553–563. <https://doi.org/10.1016/j.egypro.2012.09.029>
 90. Mauran, S., Lahmidi, H., & Goetz, V. (2008). Solar heating and cooling by a thermochemical process. First experiments of a prototype storing

- 60kWh by a solid/gas reaction. *Solar Energy*, 82(7), 623–636. <https://doi.org/10.1016/j.solener.2008.01.002>
91. Lahmidi, H., Mauran, S., & Goetz, V. (2006). Definition, test and simulation of a thermochemical storage process adapted to solar thermal systems. *Solar Energy*, 80(7), 883–893. <https://doi.org/10.1016/j.solener.2005.01.014>
 92. Tanguy, G., Marias, F., Rouge, S., Wyttenbach, J., & Papillon, P. (2012). Parametric studies of thermochemical processes for seasonal storage. *Energy Procedia*, 30, 388–394. <https://doi.org/10.1016/j.egypro.2012.11.046>
 93. Fopah-Lele, A., Rohde, C., Neumann, K., Tietjen, T., Rönnebeck, T., N'Tsoukpoe, K. E., Osterland, T., Opel, O., & Ruck, W. K. L. (2016). Lab-scale experiment of a closed thermochemical heat storage system including honeycomb heat exchanger. *Energy*, 114, 225–238. <https://doi.org/10.1016/j.energy.2016.08.009>
 94. FopahLele, A., Kuznik, F., Opel, O., & Ruck, W. K. L. (2015). Performance analysis of a thermochemical based heat storage as an addition to cogeneration systems. *Energy Convers Manag*, 106, 1327–1344. <https://doi.org/10.1016/j.enconman.2015.10.068>
 95. Ferchaud CC, Zondag HH, Boer D. Material research on salt hydrates for seasonal heat storage application in a residential environment. 2013. Available: <https://api.semanticscholar.org/CorpusID:67818386>.
 96. V. M. Essen, van, J. Cot Gores, L. P. J. Bleijendaal, H. A. Zondag, R. Schuitema, M. Bakker, and W. G. J. Helden, van, "Characterization of salt hydrates for compact seasonal thermochemical storage," in Proceedings of the 3rd ASME International Conference on Energy Sustainability (ES2009), 19–23 July 2009, San Francisco, USA, 2009, pp. 825–830. doi: <https://doi.org/10.1115/ES2009-90289>.
 97. Zondag, H., Kikkert, B., Smeding, S., de Boer, R., & Bakker, M. (2013). Prototype thermochemical heat storage with open reactor system. *Applied Energy*, 109(June), 360–365. <https://doi.org/10.1016/j.apenergy.2013.01.082>
 98. Van Essen, V. M., Zondag, H. A., Cot Gores, J., Bleijendaal, L. P. J., Bakker, M., Schuitema, R., Van Helden, W. G. J., He, Z., & Rindt, C. C. M. (2009). Characterization of MgSO₄ hydrate for thermochemical seasonal heat storage. *J Sol Energy Eng Trans ASME*, 131(4), 0410141–0410147. <https://doi.org/10.1115/1.4000275>
 99. Iammak, K., Wongsuwan, W., & Kiatsirirot, T. (2004). Investigation of modular chemical energy storage performance 2. EXPERIMENTAL SET UP. *Proc Jt Int Conf Energy Environ*, 022(December), 504–507.
 100. "Solid-sorption cooling with integrated thermal storage. The SWEAT prototype."
 101. de Boer, R., Haije, W. G., & Veldhuis, J. B. J. (2002). Determination of structural, thermodynamic and phase properties in the Na₂S–H₂O system for application in a chemical heat pump. *Thermochimica Acta*, 395(1), 3–19. [https://doi.org/10.1016/S0040-6031\(02\)00158-2](https://doi.org/10.1016/S0040-6031(02)00158-2)
 102. de Jong, A.-J., Trausel, F., Finck, C., van Vliet, L., & Cuypers, R. (2014). Thermochemical heat storage – system design issues. *Energy Procedia*, 48, 309–319. <https://doi.org/10.1016/j.egypro.2014.02.036>
 103. de Jong, A.-J., van Vliet, L., Hoegaerts, C., Roelands, M., & Cuypers, R. (2016). Thermochemical heat storage – from reaction storage density to system storage density. *Energy Procedia*, 91, 128–137. <https://doi.org/10.1016/j.egypro.2016.06.187>
 104. Henninger, S. K., Munz, G., Ratzsch, K.-F., & Schossig, P. (2011). Cycle stability of sorption materials and composites for the use in heat pumps and cooling machines. *Renewable Energy*, 36(11), 3043–3049. <https://doi.org/10.1016/j.renene.2011.03.032>
 105. Ponomarenko, I. V., Glaznev, I. S., Gubar, A. V., Aristov, Y. I., & Kirik, S. D. (2010). Synthesis and water sorption properties of a new composite 'CaCl₂ confined into SBA-15 pores'. *Microporous and Mesoporous Materials*, 129(1), 243–250. <https://doi.org/10.1016/j.micromeso.2009.09.023>
 106. Lohse, U., Liiffler, E., Kosche, K., Jänchen, J., & Parltitz, B. (1993). Isomorphous substitution of silicon in the erionite-like structure AIP04-17 and acidity of SAPO-17. *Zeolites*, 13(7), 549–556. [https://doi.org/10.1016/0144-2449\(93\)90232-R](https://doi.org/10.1016/0144-2449(93)90232-R)
 107. Rajić, N., Gabrovšek, R., Ristić, A., & Kaučič, V. (1997). Thermal investigations of some AlPO and MeAPO materials prepared in the presence of HF. *Thermochimica Acta*, 306(1), 31–36. [https://doi.org/10.1016/S0040-6031\(97\)00292-X](https://doi.org/10.1016/S0040-6031(97)00292-X)
 108. Floquet, N., Coulomb, J.-P., Dufau, N., & Andre, G. (2004). Structure and Dynamics of Confined Water in AlPO 4 -5 Zeolite. *The Journal of Physical Chemistry B*, 108, 13107–13115.
 109. Buchholz, A., Wang, W., Xu, M., Arnold, A., & Hunger, M. (2002). Thermal stability and dehydroxylation of Brønsted acid sites in silicoaluminophosphates H- SAPO-11, H- SAPO-18, H- SAPO-31, and H- SAPO-34 investigated by multi-nuclear solid-state NMR spectroscopy. *Microporous and Mesoporous Materials*, 56(3), 267–278. [https://doi.org/10.1016/S1387-1811\(02\)00491-2](https://doi.org/10.1016/S1387-1811(02)00491-2)
 110. Henninger, S. K., Schmidt, F. P., Nunez, T., & Henning, H.-M. (2005). Monte Carlo Investigations of the Water Adsorption Behavior in MFI Type Zeolites for different Si/Al Ratios with Regard to Heat Storage Applications. *Adsorption*, 11(1), 361–366. <https://doi.org/10.1007/s10450-005-5951-2>
 111. Henninger, S. K., Jeremias, F., Kummer, H., Schossig, P., & Henning, H.-M. (2012). Novel sorption materials for solar heating and cooling. *Energy Procedia*, 30, 279–288. <https://doi.org/10.1016/j.egypro.2012.11.033>
 112. Yu, N., Wang, R. Z., & Wang, L. W. (2013). Sorption thermal storage for solar energy. *Progress in Energy and Combustion Science*, 39(5), 489–514. <https://doi.org/10.1016/j.peccs.2013.05.004>
 113. Do DD. Fundamentals of Diffusion and Adsorption in Porous Media, vol. 2. 1998. https://doi.org/10.1142/9781860943829_0007.
 114. Malek, A., & Farooq, S. (1996). Comparison of isotherm models for hydrocarbon adsorption on activated carbon. *AIChE Journal*, 42(11), 3191–3201.
 115. Langmuir, I. (1916). The constitution and fundamental properties of solids and liquids. Part I. Solids. *Journal of the American Chemical Society*, 38(11), 2221–2295. <https://doi.org/10.1021/ja02268a002>
 116. J. H. Boer, The Dynamical Character of Adsorption. Clarendon P, 1968. Available: <https://books.google.co.kr/books?id=e8N4AAAAIAAJ>.
 117. Myers AL, Prausnitz JM. Thermodynamics of mixed-gas adsorption. *Aiche J*. 1965;11:121–127. Available: <https://api.semanticscholar.org/CorpusID:22369801>.
 118. Dubinin, M. M. (1960). The potential theory of adsorption of gases and vapors for adsorbents with energetically nonuniform surfaces. *Chemical Reviews*, 60(2), 235–241. <https://doi.org/10.1021/cr60204a006>
 119. Ruthven DM, Brandani S. Principles of Adsorption and Adsorption Processes, Second Edition. John Wiley & Sons, Incorporated, 2020. Available: <https://books.google.co.kr/books?id=hooRgEACAAJ>.
 120. Vijayaraghavan, K., Padmesh, T. V. N., Palanivelu, K., & Velan, M. (2006). Biosorption of nickel(II) ions onto Sargassum wightii: application of two-parameter and three-parameter isotherm models. *Journal of Hazardous Materials*, 133(1), 304–308. <https://doi.org/10.1016/j.jhazmat.2005.10.016>
 121. Kundu, S., & Gupta, A. K. (2006). Arsenic adsorption onto iron oxide-coated cement (IOCC): regression analysis of equilibrium data with several isotherm models and their optimization. *Chemical Engineering Journal*, 122(1), 93–106. <https://doi.org/10.1016/j.cej.2006.06.002>
 122. Pérez-Marín, A. B., Zapata, V. M., Ortuño, J. F., Aguilar, M., Sáez, J., & Lloréns, M. (2007). Removal of cadmium from aqueous solutions by adsorption onto orange waste. *Journal of Hazardous Materials*, 139(1), 122–131. <https://doi.org/10.1016/j.jhazmat.2006.06.008>
 123. Allen, S. J., Mckay, G., & Porter, J. F. (2004). Adsorption isotherm models for basic dye adsorption by peat in single and binary component systems. *Journal of Colloid and Interface Science*, 280(2), 322–333. <https://doi.org/10.1016/j.jcis.2004.08.078>
 124. Demirbas, E., Kobya, M., & Konukman, A. E. S. (2008). Error analysis of equilibrium studies for the almond shell activated carbon adsorption of Cr(VI) from aqueous solutions. *Journal of Hazardous Materials*, 154(1), 787–794. <https://doi.org/10.1016/j.jhazmat.2007.10.094>
 125. Ahmaruzzaman, M. (2008). Adsorption of phenolic compounds on low-cost adsorbents: a review. *Adv Colloid and Interface Sci*, 143(1), 48–67. <https://doi.org/10.1016/j.cis.2008.07.002>
 126. Abdellah, W. M., El-Ahwany, H. I., & El-Sheikh, R. (2020). Removal of Technetium (⁹⁹Tc) from Aqueous Waste by Manganese Oxide Nanoparticles Loaded into Activated Carbon. *J Anal Sci Methods Instrum*, 10(01), 12–35. <https://doi.org/10.4236/jasmi.2020.101002>
 127. Weber TW, Chakravorty RK. Pore and solid diffusion models for fixed-bed adsorbents. *Aiche J*. 1974;20:228–238. Available: <https://api.semanticscholar.org/CorpusID:98737818>
 128. Prihatiningsih, M. C., Basuki, K. T., Brawijaya, P., & Saputra, A. (2020). The adsorption isotherm and thermodynamic studies of rhenium onto mesoporous silica nanoparticles. *Journal of Physics*, 1436(1), 12124. <https://doi.org/10.1088/1742-6596/1436/1/012124>

129. Dubinin, M. M. (1947). The equation of the characteristic curve of activated charcoal. *Proc USSR Acad Sci*, 55, 327–329.
130. Thabet, M. S., & Ismaiel, A. M. (2016). Sol-Gel nanoparticles assessment of the removal of eosin yellow using: adsorption, kinetic and thermodynamic parameters. *J Encapsulation Adsorpt Sci*, 06(03), 70–90. <https://doi.org/10.4236/jeas.2016.63007>
131. M. H. Jnr. and A. I. Spiff, "Equilibrium sorption study of Al³⁺, Co²⁺ and Ag⁺ in aqueous solutions by fluted pumpkin (Telfairia occidentalis HOOK f) waste biomass," *Acta Chim. Slov.*, vol. 52, pp. 174–181, 2005. Available: <https://api.semanticscholar.org/CorpusID:21752996>.
132. A. V. Hill, "The possible effects of the aggregation of the molecules of hæmoglobin on its dissociation curves," *J. Physiol.*, vol. 40, pp. i–vii, Jan. 1910. Available: <http://jp.physoc.org/content/40/supplement/i.short>.
133. Redlich, O., & Peterson, D. L. (1959). A useful adsorption isotherm. *Journal of Physical Chemistry*, 63(6), 1024. <https://doi.org/10.1021/j150576a611>
134. Sips, R. (2004). On the structure of a catalyst surface. *The Journal of Chemical Physics*, 16(5), 490–495. <https://doi.org/10.1063/1.1746922>
135. J. Tóth, "State Equation of the Solid-Gas Interface Layers," 1971.
136. Koble, R. A., & Corrigan, T. E. (1952). adsorption isotherms for pure hydrocarbons. *Indust Eng Chem*, 44(2), 383–387. <https://doi.org/10.1021/ie50506a049>
137. Khan, A. R., Ataulh, R., & Al-Haddad, A. (1997). Equilibrium adsorption studies of some aromatic pollutants from dilute aqueous solutions on activated carbon at different temperatures. *Journal of Colloid and Interface Science*, 194(1), 154–165. <https://doi.org/10.1006/jcis.1997.5041>
138. Brunauer, S., Emmett, P. H., & Teller, E. (1938). Adsorption of gases in multimolecular layers. *Journal of the American Chemical Society*, 60(2), 309–319. <https://doi.org/10.1021/ja01269a023>
139. Hill TL. "Theory of physical adsorption," in *Advances in catalysis*, vol. 4, Elsevier, 1952, pp. 211–258.
140. McMillan, W. G., & Teller, E. (1951). The assumptions of the B.E.T. theory. *Journal of Physical Chemistry*, 55(1), 17–20. <https://doi.org/10.1021/j150484a003>
141. Freundlich H, *Over the Adsorption in Solution*, vol. 57U, no. 1. 1907. <https://doi.org/10.1515/zpch-1907-5723>.
142. Adamson AW, *Gast AP. Physical Chemistry of Surfaces*. Wiley. 1997. Available: <https://books.google.co.kr/books?id=fCyTwqLjvCUC>.
143. Haghseresht, F., & Lu, G. Q. (1998). Adsorption characteristics of phenolic compounds onto coal-reject-derived adsorbents. *Energy & Fuels*, 12(6), 1100–1107. <https://doi.org/10.1021/ef9801165>
144. Ho, Y. S., Porter, J. F., & McKay, G. (2002). Equilibrium isotherm studies for the sorption of divalent metal ions onto peat: copper, nickel and lead single component systems. *Water Air Soil Pollution*, 141(1), 1–33. <https://doi.org/10.1023/A:1021304828010>
145. Günay, A., Arslankaya, E., & Tosun, I. (2007). Lead removal from aqueous solution by natural and pretreated clinoptilolite: adsorption equilibrium and kinetics. *Journal of Hazardous Materials*, 146(1–2), 362–371. <https://doi.org/10.1016/j.jhazmat.2006.12.034>
146. Altin O, Özbelge HÖ, Dogu T. Use of General Purpose Adsorption Isotherms for Heavy Metal–Clay Mineral Interactions. *J Colloid Interface Sci*. 1998;198:130–140. Available: <https://api.semanticscholar.org/CorpusID:93823575>
147. Osagie, E., & Owabor, C. N. (2015). Adsorption of benzene in batch system in natural clay and sandy soil. *Adv Chem Eng Sci*, 05(03), 352–361. <https://doi.org/10.4236/aces.2015.53037>
148. Aharoni, C., & Ungarish, M. (1977). Kinetics of activated chemisorption. Part 2.—Theoretical models. *J Chem Soc Faraday Trans 1*, 73(0), 456–464.
149. Kim, Y., Kim, C., Choi, I., Rengaraj, S., & Yi, J. (2004). Arsenic removal using mesoporous alumina prepared via a templating method. *Environmental Science and Technology*, 38(3), 924–931. <https://doi.org/10.1021/es0346431>
150. Krishna Prasad, R., & Srivastava, S. N. (2009). Sorption of distillery spent wash onto fly ash: Kinetics and mass transfer studies. *Chemical Engineering Journal*, 146(1), 90–97. <https://doi.org/10.1016/j.cej.2008.05.021>
151. Ng, J. C. Y., Cheung, W. H., & McKay, G. (2002). Equilibrium studies of the sorption of Cu(II) ions onto chitosan. *Journal of Colloid and Interface Science*, 255(1), 64–74. <https://doi.org/10.1006/jcis.2002.8664>
152. Gimbert, F., Morin-Crini, N., Renault, F., Badot, P.-M., & Crini, G. (2008). Adsorption isotherm models for dye removal by cationized starch-based material in a single component system: error analysis. *Journal of Hazardous Materials*, 157(1), 34–46. <https://doi.org/10.1016/j.jhazmat.2007.12.072>
153. Wong, Y. C., Szeto, Y. S., Cheung, W. H., & McKay, G. (2004). Adsorption of acid dyes on chitosan—equilibrium isotherm analyses. *Process Biochemistry*, 39(6), 695–704. [https://doi.org/10.1016/S0032-9592\(03\)00152-3](https://doi.org/10.1016/S0032-9592(03)00152-3)
154. Khan, A. R., Al-Waheab, I. R., & Al-Haddad, A. (1996). A generalized equation for adsorption isotherms for multi-component organic pollutants in dilute aqueous solution. *Environmental Technology*, 17(1), 13–23. <https://doi.org/10.1080/09593331708616356>
155. Langmuir, I. (1918). The adsorption of gases on plane surfaces of glass, mica and platinum. *Journal of the American Chemical Society*, 40(9), 1361–1403. <https://doi.org/10.1021/ja02242a004>
156. Dubinin, M. M. (1967). Adsorption in micropores. *Journal of Colloid and Interface Science*, 23(4), 487–499. [https://doi.org/10.1016/0021-9797\(67\)90195-6](https://doi.org/10.1016/0021-9797(67)90195-6)
157. Parker, G. R. (1995). Optimum isotherm equation and thermodynamic interpretation for aqueous 1,1,2-trichloroethene adsorption isotherms on three adsorbents. *Adsorption*, 1(2), 113–132. <https://doi.org/10.1007/BF00705000>
158. Cook, W. H., & Basmadjian, D. (1964). Correlation of adsorption equilibria of pure gases on activated carbon. *Canadian Journal of Chemical Engineering*, 42(4), 146–151. <https://doi.org/10.1002/cjce.5450420403>
159. Nikolaev, K. M., & Dubinin, M. M. (1958). Concerning adsorption properties of carbon adsorbents 3. A study of adsorption isotherms of gases and vapors on active carbons over a wide interval of temperatures, including the critical region. *Bull Acad Sci USSR, Div Chem Sci*, 7(10), 1124–1133. <https://doi.org/10.1007/BF00914939>
160. Nagel, T., Beckert, S., Böttcher, N., Gläser, R., & Kolditz, O. (2015). The impact of adsorbate density models on the simulation of water sorption on nanoporous materials for heat storage. *Energy Procedia*, 75, 2106–2112. <https://doi.org/10.1016/j.egypro.2015.07.331>
161. Nagel, T., Beckert, S., Lehmann, C., Gläser, R., & Kolditz, O. (2016). Multi-physical continuum models of thermochemical heat storage and transformation in porous media and powder beds—A review. *Applied Energy*, 178, 323–345. <https://doi.org/10.1016/j.apenergy.2016.06.051>
162. Aristov, Y. I., Glaznev, I. S., Freni, A., & Restuccia, G. (2006). Kinetics of water sorption on SWS-1L (calcium chloride confined to mesoporous silica gel): Influence of grain size and temperature. *Chemical Engineering Science*, 61(5), 1453–1458. <https://doi.org/10.1016/j.ces.2005.08.033>
163. Glueckauf, E. (1955). Theory of chromatography. Part 10.—Formulæ for diffusion into spheres and their application to chromatography. *Transactions of the Faraday Society*, 51, 1540–1551. <https://doi.org/10.1039/TF9555101540>
164. Westwater, J. W., & Drickamer, H. G. (1957). The Mathematics of Diffusion. *Journal of the American Chemical Society*, 79(5), 1267–1268. <https://doi.org/10.1021/ja01562a072>
165. Chua, H. T., Ng, K. C., Wang, W., Yap, C., & Wang, X. L. (2004). Transient modeling of a two-bed silica gel–water adsorption chiller. *International Journal of Heat and Mass Transfer*, 47(4), 659–669. <https://doi.org/10.1016/j.jijheatmasstransfer.2003.08.010>
166. Lee C-H. *Adsorption science and technology*. World Scientific. 2003. <https://doi.org/10.1142/5257>.
167. Valenciano, R., Aylón, E., & Izquierdo, M. T. (2015). A critical short review of equilibrium and kinetic adsorption models for vocs breakthrough curves modelling. *Adsorp Sci Technol*, 33(10), 851–870. <https://doi.org/10.12660/0263-6174.33.10.851>
168. Whitaker, S. (1986). Flow in porous media I: a theoretical derivation of Darcy's law. *Transport in Porous Media*, 1(1), 3–25. <https://doi.org/10.1007/BF01036523>
169. "Che Eng Pro48, 89.pdf"
170. Ergun S. Fluid flow through packed columns. 1952. Available: <https://api.semanticscholar.org/CorpusID:135806248>.
171. Solmuş, S. I., Rees, D. A. S., Yamali, C., Baker, D., & Kaftanoğlu, B. (2012). Numerical investigation of coupled heat and mass transfer inside the adsorbent bed of an adsorption cooling unit. *International Journal of Refrigeration*, 35(3), 652–662. <https://doi.org/10.1016/j.jirefrig.2011.12.006>

172. Alam, K. C. A., Saha, B. B., Kang, Y. T., Akisawa, A., & Kashiwagi, T. (2000). Heat exchanger design effect on the system performance of silica gel adsorption refrigeration systems. *International Journal of Heat and Mass Transfer*, 43(24), 4419–4431. [https://doi.org/10.1016/S0017-9310\(00\)00072-7](https://doi.org/10.1016/S0017-9310(00)00072-7)
173. Mahdavihah, M., & Niazmand, H. (2013). Effects of plate finned heat exchanger parameters on the adsorption chiller performance. *Applied Thermal Engineering*, 50(1), 939–949. <https://doi.org/10.1016/j.applthermaleng.2012.08.033>
174. Mitra, S., Srinivasan, K., Kumar, P., Murthy, S. S., & Dutta, P. (2014). Solar driven adsorption desalination system. *Energy Procedia*, 49, 2261–2269. <https://doi.org/10.1016/j.egypro.2014.03.239>
175. Mitra, S., Kumar, P., Srinivasan, K., & Dutta, P. (2014). Simulation study of a two-stage adsorber system. *Applied Thermal Engineering*, 72(2), 283–288. <https://doi.org/10.1016/j.applthermaleng.2014.04.023>
176. Chua, H. T., Ng, K. C., Malek, A., Kashiwagi, T., Akisawa, A., & Saha, B. B. (1999). Modeling the performance of two-bed, silica gel-water adsorption chillers. *International Journal of Refrigeration*, 22(3), 194–204. [https://doi.org/10.1016/S0140-7007\(98\)00063-2](https://doi.org/10.1016/S0140-7007(98)00063-2)
177. Chakraborty, A., Saha, B. B., & Aristov, Y. I. (2014). Dynamic behaviors of adsorption chiller: effects of the silica gel grain size and layers. *Energy*, 78, 304–312. <https://doi.org/10.1016/j.energy.2014.10.015>
178. Allouhi, A., Kousksou, T., Jamil, A., & Zeraoui, Y. (2014). Modeling of a thermal adsorber powered by solar energy for refrigeration applications. *Energy*, 75, 589–596. <https://doi.org/10.1016/j.energy.2014.08.022>
179. Freni, A., Maggio, G., Cipiti, F., & Aristov, Y. I. (2012). Simulation of water sorption dynamics in adsorption chillers: one, two and four layers of loose silica grains. *Applied Thermal Engineering*, 44(February 2016), 69–77. <https://doi.org/10.1016/j.applthermaleng.2012.03.038>
180. Demir H, Mobedi M, Ulku S. Effects of porosity on heat and mass transfer in a granular adsorbent bed ★. *Int Commun Heat Mass Transf.* 2009;36. <https://doi.org/10.1016/j.icheatmasstransfer.2009.01.008>.
181. Riffel, D. B., Wittstadt, U., Schmidt, F. P., Núñez, T., Belo, F. A., Leite, A. P. F., & Ziegler, F. (2010). Transient modeling of an adsorber using finned-tube heat exchanger. *International Journal of Heat and Mass Transfer*, 53(7), 1473–1482. <https://doi.org/10.1016/j.ijheatmasstransfer.2009.12.001>
182. Sun, L. M., Ben Amar, N., & Meunier, F. (1995). Numerical study on coupled heat and mass transfers in an absorber with external fluid heating. *Heat Recover Syst CHP*, 15(1), 19–29. [https://doi.org/10.1016/0890-4332\(95\)90034-9](https://doi.org/10.1016/0890-4332(95)90034-9)
183. Narayanan S, Li X, Yang S, McKay I, Kim H, Wang E. Design and Optimization of High Performance Adsorption-Based Thermal Battery. 2013. <https://doi.org/10.1115/HT2013-17472>.
184. Narayanan, S., Yang, S., Kim, H., & Wang, E. (2014). Optimization of adsorption processes for climate control and thermal energy storage. *International Journal of Heat and Mass Transfer*, 77, 288–300. <https://doi.org/10.1016/j.ijheatmasstransfer.2014.05.022>
185. Narayanan, S., Li, X., Yang, S., Kim, H., Umans, A., McKay, I. S., & Wang, E. N. (2015). Thermal battery for portable climate control. *Applied Energy*, 149, 104–116. <https://doi.org/10.1016/j.apenergy.2015.03.101>
186. Tatsidjodoung P, Le Pierrès N, Heintz J, Lagre D, Luo L, Durier F. Experimental and numerical investigations of a zeolite 13X/water reactor for solar heat storage in buildings. *Energy Convers Manag.* 488–500. <https://doi.org/10.1016/j.enconman.2015.11.011>.
187. Hu, P., Yao, J.-J., & Chen, Z.-S. (2009). Analysis for composite zeolite/foam aluminum–water mass recovery adsorption refrigeration system driven by engine exhaust heat. *Energy Convers Manag*, 50(2), 255–261. <https://doi.org/10.1016/j.enconman.2008.09.022>
188. Weber, R., Kerskes, H., & Drück, H. (2014). Development of a combined hot water and sorption store for solar thermal systems. *Energy Procedia*, 48, 464–473. <https://doi.org/10.1016/j.egypro.2014.02.055>
189. Nakaso, K., Tanaka, Y., Eshima, S., Kobayashi, S., & Fukai, J. (2015). Performance of a novel steam generation system using a water-zeolite pair for effective use of waste heat from the iron and steel making process. *ISIJ International*, 55, 448–456. <https://doi.org/10.2355/isijinternational.55.448>
190. Kamdem, S. M., Johannes, K., Kuznik, F., Bouia, H., & Roux, J.-J. (2014). Sensitivity analysis of the energy density in a thermo chemical heat storage device. *Energy Procedia*, 48, 405–412.
191. Restuccia, G., Freni, A., & Maggio, G. (2002). A zeolite-coated bed for air conditioning adsorption systems: parametric study of heat and mass transfer by dynamic simulation. *Applied Thermal Engineering*, 22(6), 619–630. [https://doi.org/10.1016/S1359-4311\(01\)00114-4](https://doi.org/10.1016/S1359-4311(01)00114-4)
192. Freni, A., Bonaccorsi, L., Proverbio, E., Maggio, G., & Restuccia, G. (2009). Zeolite synthesised on copper foam for adsorption chillers: a mathematical model. *Microporous Mesoporous Materials*, 120, 402–409. <https://doi.org/10.1016/j.micromeso.2008.12.011>
193. Marletta, L., Maggio, G., Freni, A., Ingrassiotta, M., & Restuccia, G. (2002). A non-uniform temperature non-uniform pressure dynamic model of heat and mass transfer in compact adsorbent beds. *International Journal of Heat and Mass Transfer*, 45(16), 3321–3330. [https://doi.org/10.1016/S0017-9310\(02\)00045-5](https://doi.org/10.1016/S0017-9310(02)00045-5)
194. Maggio, G., Freni, A., & Restuccia, G. (2006). A dynamic model of heat and mass transfer in a double-bed adsorption machine with internal heat recovery. *International Journal of Refrigeration*, 29(4), 589–600. <https://doi.org/10.1016/j.ijrefrig.2005.10.005>
195. Wu, W., Zhang, H., & Sun, D. (2009). Mathematical simulation and experimental study of a modified zeolite 13X–water adsorption refrigeration module. *Applied Thermal Engineering*, 29, 645–651.
196. Ryu, Y. K., Lee, S. J., Kim, J. W., & Lee, C. H. (2001). Adsorption equilibrium and kinetics of H₂O on Zeolite 13X. *Korean Journal of Chemical Engineering*, 18(4), 525–530. <https://doi.org/10.1007/BF02698301>
197. Ma, Z., Bao, H., & Roskilly, A. P. (2019). Seasonal solar thermal energy storage using thermochemical sorption in domestic dwellings in the UK. *Energy*, 166, 213–222. <https://doi.org/10.1016/j.energy.2018.10.066>
198. Yue, X., Xu, Y., Zhou, X., Xu, D., & Chen, H. (2022). Study on the performance of a solar heating system with seasonal and cascade thermal-energy storage. *Energies*, 15, 20. <https://doi.org/10.3390/en15207733>
199. Crespo, A., Fernández, C., de Gracia, A., & Frazzica, A. (2022). Solar-driven sorption system for seasonal heat storage under optimal control: study for different climatic zones. *Energies*, 15, 15. <https://doi.org/10.3390/en15155604>
200. Jiang L, Liu W, Lin YC, Wang RQ, Zhang XJ, Hu MK. Hybrid thermo-chemical sorption seasonal storage for ultra-low temperature solar energy utilization. *Energy.* 2022;239. <https://doi.org/10.1016/j.energy.2021.122068>.

Publisher's Note

Springer Nature remains neutral with regard to jurisdictional claims in published maps and institutional affiliations.